Winter 12-15-2023

EXPLORING SOYBEAN OIL-BASED POLYOL AND EFFECT OF NON-HALOGENATED FLAME RETARDANTS IN RIGID POLYURETHANE FOAM

Sahithi Kondaveeti
Pittsburg State University, skondaveeti@gus.pittstate.edu

EXPLORING SOYBEAN OIL-BASED POLYOL AND THE EFFECT OF NON-HALOGENATED FLAME RETARDANTS IN RIGID POLYURETHANE FOAM

Thesis Submitted to the Graduate School
in Partial Fulfilment of the Requirements
For the Degree of
Master of Science

Sahithi Kondaveeti

Pittsburg State University

Pittsburg, Kansas

December, 2023

EXPLORING SOYBEAN OIL-BASED POLYOL AND THE EFFECT OF NON-HALOGENATED FLAME RETARDANTS IN RIGID POLYURETHANE FOAM

Sahithi Kondaveeti

APPROVED:

Thesis Advisor _____
Dr. Ram K. Gupta, Department of Chemistry

Committee Member _____
Dr. Khamis Siam, Department of Chemistry

Committee Member _____
Dr. Timothy Dawsey, National Institute for Materials Advancement

Acknowledgments

I would like to express my heartfelt gratitude to all those who have contributed to the completion of this thesis. First and foremost, I am deeply thankful to my supervisor, Dr. Ram K. Gupta, for his unwavering support, guidance, and invaluable insights throughout the research process. His expertise and encouragement have been instrumental in shaping this work. His dedication to excellence and commitment to fostering a rigorous academic environment have greatly enriched my research experience. I am profoundly grateful for Dr. Gupta's time and effort in reviewing and advising on my work, shaping it into a more comprehensive and refined piece. I appreciate his unwavering support, which has been instrumental in my academic growth.

I extend my appreciation to the faculty members for their constructive feedback and scholarly input, which greatly enriched the quality of this thesis. I am grateful to my family for their constant encouragement, love, and understanding during the challenging times of this academic journey. Their belief in my abilities has been a driving force behind my success. Special thanks to my friends and peers who provided not only academic assistance but also moral support, creating a positive and motivating environment for me to thrive. I also want to acknowledge the Department of Chemistry, and the National Institute for Materials Advancement, Pittsburg State University for providing financial support that facilitated the execution of this research. This thesis would not have been possible without the collective support of these individuals and organizations. Thank you for being an integral part of this academic endeavor.

EXPLORING SOYBEAN OIL-BASED POLYOL AND THE EFFECT OF NON-HALOGENATED FLAME RETARDANTS IN RIGID POLYURETHANE FOAM

An Abstract of the Thesis by
Sahithi Kondaveeti

To address the increasing demand for sustainable biomaterials due to the depletion of fossil fuel resources and growing environmental concerns, a new type of biodegradable and environmentally friendly rigid polyurethane foam (RPUF) has been synthesized. These foams are derived from chemically modified soybean oil-based polyol obtained from soybean oil by epoxidation followed by a ring-opening reaction. Polyurethane foam is generally used in construction, furniture, and automobile industries but is highly flammable and releases toxic gases and smoke during combustion. In this study, a highly efficient synergistic effect halogen-free flame-retardant (FR) melamine salt, 2-carboxyethyl(phenyl)phosphinic acid melamine salt (CMA) was synthesized from 2-carboxyethyl(phenyl)phosphinic acid (CEPP) and Melamine (MA) in aqueous solution. Fourier transform infrared (FT-IR) spectroscopy characterized the chemical structure of CMA. Three different FRs, Melamine (MA), Melamine Cyanurate (MC), and 2-carboxyethyl(phenyl)phosphinic acid melamine salt (CMA) was (separately) introduced in increasing quantities for the foam preparation to suppress the flame during combustion. The effects of these flame retardants on the mechanical properties, flame retardancy, thermal stability, and morphology of the prepared RPUFs were studied by apparent density, closed cell content, compression test, horizontal burning test, thermogravimetric analysis (TGA), gel permeation chromatography (GPC), and scanning electron microscopy (SEM). The addition of 28.56 wt % of MA (MA-15), MC (MC-15), and CMA (CMA-15) showed a burning time of 10.1 sec with weight loss of

5.34% and 28.4 sec with 13.02% and 15.25 sec with 8%, respectively. The findings demonstrated that all three FRs gave RPUF good flame-retardant properties, but MA derivatives (MC and CMA) showed lesser effect when compared to MA. Overall, the usage of SBO-polyol did not change most of the foam's qualities. As a result, our research on the synthesis of biobased flame retardant RPUFs was successful.

TABLE OF CONTENTS

LIST OF TABLES

LIST OF FIGURES

LIST OF ABBREVIATIONS

PU	Polyurethane
RPUF	Rigid polyurethane foam
SBO	Soybean oil
ESBO	Epoxidized soybean oil
FR	Flame Retardant
MA	Melamine
MC	Melamine cyanurate
CEPP	2-Carboxyethyl(phenyl)phosphinic acid
CMA	2-Carboxyethyl(phenyl)phosphinic acid melamine salt
MDI	Methylene diphenyl diisocyanate
FTIR	Fourier transformed infrared
TGA	Thermogravimetric analysis
DTGA	Derivative thermogravimetric analysis
GPC	Gel permeation chromatography
SEM	Scanning electron microscopy
CCC	Closed cell content
ASTM	American Society for Testing and Materials
ISO	International Organization for Standardization

CHAPTER I

INTRODUCTION

1.1. Polyurethane: Background and Overview

Dr. Otto Bayer and his colleagues made a substance known as "Das Di-lsocganat-Poluadditionsverfahren," or polyurethane, in the years leading up to World War II (1937). Little did they know that this discovery at IG Farben in Leverkusen, Germany, would further alter the world of materials and engineering. Comparing polyurethane to its modern counterparts, it is significantly more versatile and diverse in many ways. Because of its superior qualities and ease of production, polyurethane is one of the most sought-after polymers. Initially created as a substitute for the elastic rubber utilized in World War II, its versatility led to its rapid replacement of other materials such as metals and woven fibers [1], [2]. Polyurethane (PU) is a plastic polymer consisting of repeating units containing a urethane group. Demand for PU has increased because of its properties such as high strength-to-weight ratio, insulation, soundproofing, lightweight, low thermal conductivity, versatility, and durability [3]. Since its introduction to the market, the polyurethane material has been a revelation in and of itself. It has developed into binders, coatings, paints, elastomers, and foams (flexible and rigid). It is among the best-performing materials for footwear, furniture, automotive interiors, buildings, packaging, and thermal insulation, among other uses.

1.2. Basic Chemistry of Polyurethane

Polyurethane is created through the interaction of di/poly isocyanate with a diol or polyol, generating repeated urethane linkages, in the presence of a chain extender and other additives. Understanding the structure-property relationship between polyol and isocyanate is essential for creating and designing polyurethane products, as altering either one can result in significant changes to the polyurethane's qualities [4]. In general, polyols are pliable sections of the polymeric chain that support the elasticity shown by polyurethanes. The overabundance of polyols results in final polyurethanes that are typically softer and more hydrophilic. Due to their higher reactivity, role in the curing process, and ability to form the rigid portion of polyurethanes, isocyanates can be added in excess to produce polyurethanes that are more rigid and hydrophobic [5]. By simply altering the quantity and types of polyol, isocyanate, or additives, PUs can be produced in any way and have a wide range of qualities, including density and hardness.

1.3. Classification of Polyurethane

Because polyurethanes are so versatile, it is difficult to classify them simply by name. **Figure 1** presents the most effective means of characterizing and categorizing all the formats.

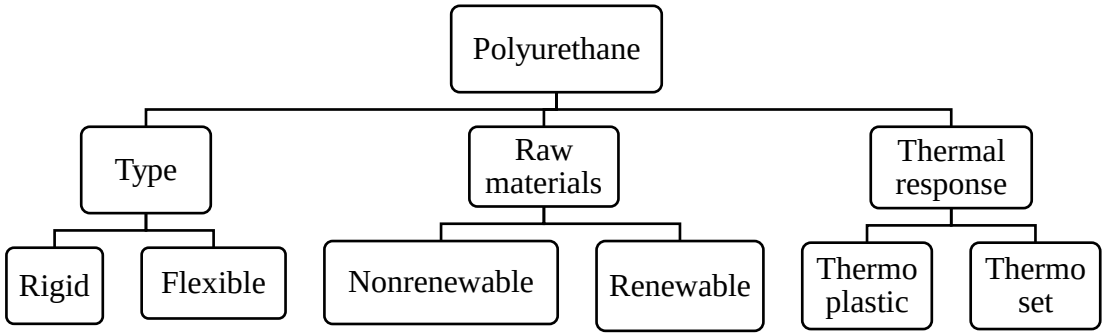

Figure 1. Classification of polyurethane.

1.3.1. Types of Polyurethane

PUs can be classified as rigid, flexible, thermoplastic, waterborne, adhesives, coating, binders, elastomers, and sealants due to the wide range of sources from which they can be synthesized and their unique applications [6]. One of the most well-known, adaptable, and energy-saving insulations is rigid polyurethane foam. In addition to improving the comfort and efficiency of commercial and household appliances, these foams have the potential to drastically lower energy expenses. These foams have demonstrated their efficacy as insulating materials, finding use in window, wall, and roof insulations, as well as in air and door barrier sealants. Certain block copolymers, known as flexible PU foams, are so named because of the phase separations that occur between the soft and hard segments [7]. Flexible polyurethane foams are used as cushioning materials in many kinds of consumer and business goods. This covers the following: car interior components, packaging, underlays for carpets, furniture, bedding, etc. Polyols have short chains, high functionality, and aromatic segments in

their structure, and more than 90% of closed cells are typically used to create rigid polyurethanes. Flexible polyurethanes, on the other hand, have an open-cell structure that permits air to flow freely. Rigid foams, which have around 90% closed cells, are utilized for good thermal insulation in refrigerators, buildings, and homes because they prevent the flow of heat and air [5].

1.3.2. Raw Materials

Various methods can be used to manufacture PUs. The most significant and practical technique involves the interaction of a diisocyanate with a polyol, which is an alcohol molecule containing two or more hydroxyl groups. The polyurethane sector depends on feedstocks derived from petroleum. The use of resources derived from petroleum poses a few challenges, including the product's low thermal resistance, the depletion of global fossil reserves, environmental concerns, and the volatile price of crude oil. Instead of using synthetic materials, a lot of work has been done recently to produce sustainable alternatives. The formulation of bio-mass polyols has been successful, even though isocyanate has not yet been synthesized from bio-based resources. The need for non-petroleum-based products has grown in the last few decades because of cheap costs, significant environmental concerns, and regulatory regulations. For the manufacture of biobased polyols, many renewable feedstocks, including fatty acids, vegetable oils, and resources based on protein [8].

1.3.3. Thermal Response

Based on how they react to thermal energy, polyurethanes can be classified as thermosets or thermoplastic materials. Thermoset materials create network architectures through chemical crosslinking. Thermoset elastomers are molded using

casting procedures; once formed, they cannot be reshaped because they become set when heated. Additionally, they can withstand higher temperatures without losing structural integrity because of their higher melting point [9]**.** Thermoplastic materials, in contrast to thermosets, can be remolded without undergoing any chemical modifications. Heat can be applied to them to soften and melt them. When crosslink bonds develop, thermoplastic polyurethanes can undergo processing and change into thermoset form. Interestingly, there is a threefold greater market demand for thermosets manufacture than there is for thermoplastic materials [10]. The mechanical characteristics (tensile and compressive strength, and hardness) of thermosetting polymers are not affected by temperature like those of thermoplastics.

1.4. Applications of Polyurethanes

The polyol and isocyanate that have been utilized have a significant impact on the physical and chemical characteristics of PU. Most of the time, 60–70% of a polyurethane's quality depends on the kind that was utilized. Modifying the polymer's chain length, molecular structure, functionality, and functionalization of the polyol chain with substances like fluorine, acrylics, or rubbers can significantly change the polymer's properties. Polyurethane offers an advantage over other materials in many industrial applications because of this level of customization. It has many uses and is difficult to classify because of the wide range of tunability permitted in polyurethane chemistry. With around 37% of the PU foam industry being produced, flexible polyurethane foams hold the largest market share [11]. The most common kind, they are used for specialized purposes such as mattresses, couches, car seats, and car interior design. They are also used for some medical devices. They are utilized in medical

applications such as tubing, surgical drapes, catheters, hospital beds, wound dressings, and various other uses because of their availability, good mechanical qualities, and biocompatibility. It is preferable to use alternative water-borne polyurethanes for elastomeric and sealant applications [6], [12]. Because of their unique advantages, rigid foams are the second most popular PU. When used for thermal insulation in buildings, they can offer insulation and are very helpful for preserving energy [13]. They can be applied on automotive, aerospace, wood, textile, and glass topcoats and finishes in the coatings business. Their low moisture permeability, strong mechanical advantage, resistance to corrosion, and chemical resistance are the reasons for this [14]. Adhesives made of polyurethane are strong, resistant to solvents, cohesive, and abrasion-resistant. As a result, they are used in wood flooring, rotor blades, construction, automobiles, and industrial settings [15]. **Figure 2** illustrates how polyurethanes are used in several sectors.

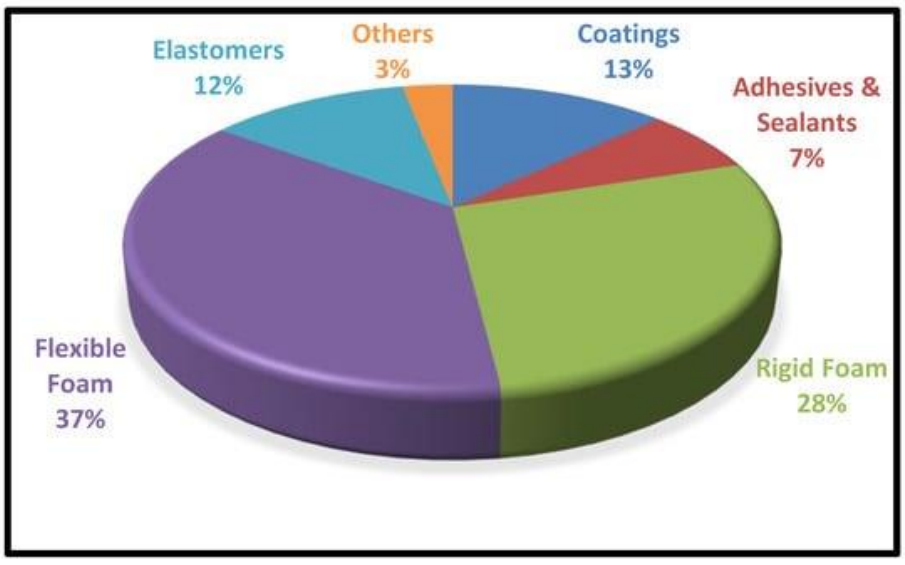

Figure 2. Global consumption of polyurethanes. Reproduced with permission [16]. Copyright (2022), Multidisciplinary Digital Publishing Institute.

1.5. Issues of Polyurethane Foams

Rigid polyurethane foams have many desirable fashionable qualities, but because of their high surface area, low thermal inertia, porosity (open-cell porous structure), low density, and cellular structure, they are extremely combustible when used for soft furnishings and insulation [17]–[19]. Due to oxygen deprivation in fire victims, dangerous gases such as CO, CO_2, and HCN created by burning polyurethane foams also have poisoning and suffocating consequences. Furthermore, the thick smoke makes it harder to see, which hinders the timely evacuation and rescue of those who are stuck. Low heat stability and significant smoke generation have been discovered to be related to the structure and composition of polyurethane. As a result, there is more thought being given to changing the polyurethane matrix. For example, it has been found that the presence of aromatic groups in the backbone lowers the amount of smoke produced and encourages the production of char, which lowers flammability. Furthermore, flame retardants have been studied extensively and applied to lower polyurethane foams' high rate of combustion [20].

Another significant issue facing the polyurethane industry is the use of polyols derived from petrochemical sources in the synthesis of polyurethanes. As a result, steps are being taken to find economical, biobased, and renewable sources of valuable polyols [21]. Isocyanate, which is created from the dangerous chemical phosgene, is another problem with the manufacture of polyurethanes. Long-term isocyanate exposure has negative consequences on the respiratory system and other body systems [22], [23].

1.6. Polyol

Polyols with two or more -OH groups are frequently utilized in the synthesis of PU. Polyols make up most of the starting materials that can be synthesized to create polyurethanes with a variety of characteristics. High and low-molecular-weight polyols are the two primary categories into which they can be divided. The nature, functionality, and molecular weight of the polyols influence the polyurethanes' qualities. Flexible and semi-flexible foams, adhesives, coatings, elastomers, sealants, and other goods made primarily of elastic polyurethanes account for over 70% of the polyurethane produced globally. Because of their linear chains, which permit unrestricted rotation along with low functionality (2-4) and low degree of cross-linking, high molecular weight polyols with long alkyl segments are utilized to prepare flexible or elastic polyurethanes. Low molecular weight polyols provide another significant class of precursor chemicals for the synthesis of rigid polyurethanes [24]. Their short chains and high functionality (3–8) raise their viscosity, resulting in highly branched and cross-linked polyurethanes. Furthermore, rigidly structured polyurethanes are produced via their interaction with aromatic isocyanates, such as diphenyl methylene diisocyanate. There are more interactions between the chains when there are several urethane connections resulting from the presence of hydroxyl groups [5].

The most common polyols for flexible polyurethanes are polyalkylene oxide polyether polyols. The second most produced polyol for polyurethanes is polyester polyol. Comparing polyester-based polyurethanes to polyether-based polyurethanes, it is known that the former exhibits better fire resistance, higher thermal stability, and higher crystallinity (because of stronger intermolecular contacts between polymeric

chains). Another class of polyols that are frequently employed in the production of polyurethanes is acrylic polyols. To react with isocyanate, at least one of the monomers needs to have a hydroxyalkyl group present [5].

Because polyurethanes are widely produced using petrochemical-based raw materials, there are considerations regarding how to employ alternative sources that could ensure more reliable and affordable production while also addressing environmental concerns and economic volatility. The depletion of global fossil fuels, environmental concerns, the product's low thermal resistance, and the price volatility of crude oil are only a few of the challenges that arise with the consumption of petroleum-based resources. A growing understanding of these factors has led to the discovery of numerous promising biopolymers in the field of renewable materials research. Saturated and/or unsaturated fatty acids, which comprise more than 90% fatty acid components, as well as a significant proportion of triglyceride-based fatty acids compose the main chain of plant oils, which are present in nature. Several bioderived starting materials, including glycerol, sorbitol, sucrose, and ricinoleic acid (which is derived from castor oil triglyceride), include naturally occurring hydroxyl groups. These materials can be utilized directly to produce polyurethane. Vegetable oils [25], fruit oils, and other plant-based derivatives [26] are examples of other biomaterials that are readily transformed into polyols for polyurethanes. They are affordable, easily obtainable, environmentally friendly, and extremely sustainable. As a result, more natural oils are being used in the synthesis of bio-based polyols [27], [28]. To create bio-based polyols, numerous scientific endeavors have been carried out employing plant oils such as soybean, sunflower [29], [30], cardanol, castor [31], [32], and

rapeseed oil [3]. There are several ways to synthesize the bio polyols, including epoxidation followed by ring-opening [33], ozonolysis, transesterification, and thiol-ene reactions [34]. Lignin [35], terpenes [36], terpenoids, and maize are a few examples of beginning materials that have been transformed into biopolyols.

1.7. Isocyanate

Another important ingredient in the manufacture of various polyurethane compounds is isocyanates. **Figure 3**'s resonance structures illustrate the unstable nature of the NCO groups in isocyanate, which accounts for their high reactivity. After carbon, oxygen has a greater electron density than nitrogen. Nitrogen will have an intermediate negative charge, carbon a positive charge, and oxygen a negative charge in its intermediate form. Hydrogen is added to the NCO group as a result of a chemical reaction in which the electrophilic center of the carbon in isocyanate is attacked by the nucleophilic center of oxygen from the hydroxyl group (OH) in the polyol [24], [37]. Equal amounts of reactive groups must be present for the polyurethane monomers, polyol (OH) and isocyanate (NCO), to undergo a complete reaction. To react with any moisture present, the isocyanate is usually added in excess in practical operations. This results in the formation of an unstable carbamic acid, which breaks down into carbon dioxide and an amine (**Figure 4B**). The carbon dioxide produced is useful for polyurethane foams' cellular structure's development and expansion [24], [38]. As seen in **Figure 4C**, the amine might further react with excess isocyanate to create urea [39]. On the other hand, the primary polyurethane structure can also contain additional moieties such as urea, ester, ether, and aromatic groups in addition to numerous urethane connections [40], [41].

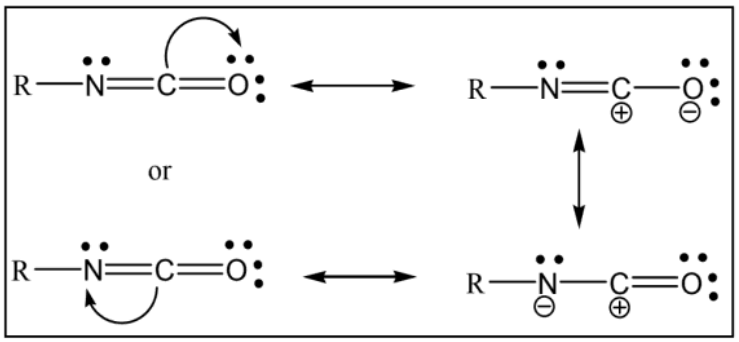

Figure 3. Illustration of resonance structures of isocyanate. Reproduced with permission [42]. Copyright 2012, InTech.

Since their NCO group's carbon-nitrogen double bond is crossed by a nucleophilic addition, they are extremely reactive to nucleophiles that carry protons [41]. Conversely, isocyanates, despite their slowness at room temperature, are included in PU production with compounds containing hydroxyl groups because of their strong reactivity [10]. The phase mismatch between the comparatively non-polar and denser isocyanate phase and the polar and less dense polyol phase could be the cause of the poor pace. Aliphatic isocyanates like isophorene diisocyanate (IPDI) and hexamethylene diisocyanate (HDI) are less reactive than their aromatic counterparts like toluene diisocyanate (TDI) and diphenylmethane diisocyanate (MDI). A small number of isocyanates, like diphenylmethane diisocyanate, are difunctional, meaning that each molecule has two isocyanate groups. Other isocyanates are composed of combinations of molecules that have two or more isocyanate groups [6]. Aromatic isocyanates are more reactive than their aliphatic counterparts due to the delocalization of negative charges on the aromatic rings, which is based on their structures [38]. Applications with high modulus, glass transitions, and tensile strength are usually the outcome of aromatic isocyanates. Conversely, aliphatic isocyanates are better suited for

coatings, elastomers, or rubbers that need low tensile strength and a high elongation break [37], [43]. Even while isocyanates have many advantageous properties, there are related environmental and health risks. Consequently, chronic human exposure to isocyanate has been linked to harmful, pulmonary, and carcinogenic effects, according to experts [44]. To overcome this, scientists have embarked on a replacement endeavor, producing non-isocyanate polyurethanes (NIPU) by employing several synthesis techniques [45], [46].

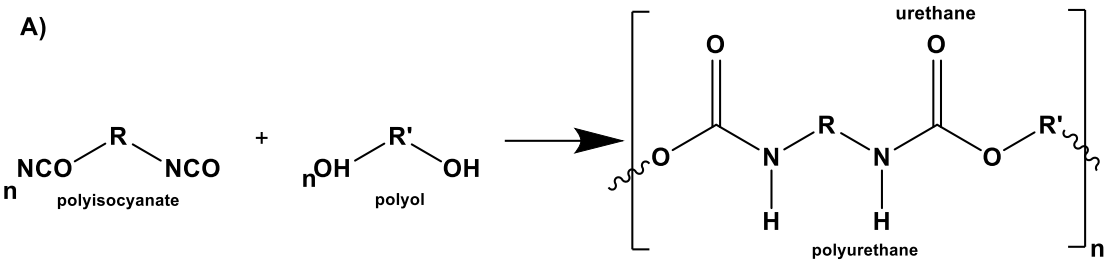

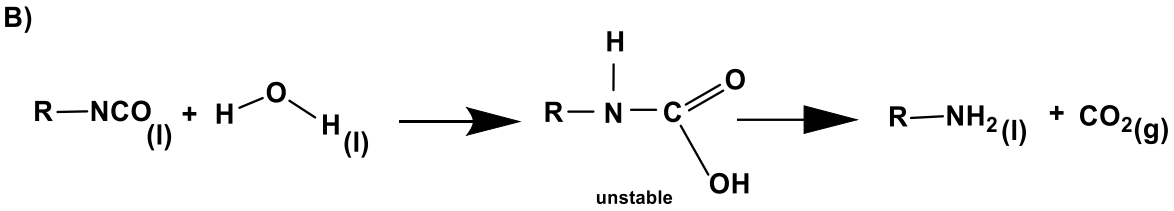

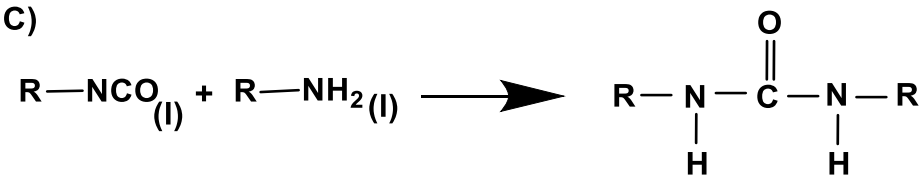

Figure 4. A) Reaction between isocyanate and polyol. **B)** Reaction of isocyanate with water. **C)** Reaction of isocyanate with amine. Adapted with permission [39]. Copyright (2010), American Chemical Society.

1.8. Flame-Retardants

PU foam has a high burning velocity and is very simple to ignite. This is brought about by the polymer matrix's open cell structure, low aromaticity, high surface-to-mass ratio, and high air permeability as well as high oxygen, carbon, and hydrogen content. The exothermic reaction that breaks down polyurethane releases a lot of poisonous and dangerous gases, such as NO_x, CO, HCN, N_2, and H_2O. Consequently, a significant problem with polyurethane foams is their flammability, which can be mitigated by adding flame retardants.

Flame-retardants (FR) are compounds that fall into two groups. During prepolymer preparation, ingredients are physically combined to form the first type of additive FR. These are not part of the polyurethane's chemical structure. Due to its ease of use, cheaper cost, overall effectiveness, and lack of an active site on the FR molecule that would allow for chemical association with the polymeric matrix, additive FR is used in most processes. The second group is reactive FR. Here, the FR molecule is added to the polymeric structure chemically. It raises the cost by introducing an additional synthetic phase. Nonetheless, to obtain efficient FR characteristics, smaller concentrations of reactive FR are typically needed. Additionally, the polyurethane's FR active molecules are dispersed more uniformly, enabling the foam to exhibit consistent flame retardancy [47], [48].

FRs are also categorized into those that contain halogen and that is halogen-free, such as phosphate, nitrogen, nitrogen-phosphorus, silicon, boron, and antimony compounds, sulfate, expandable graphite, nano composites like fullerene, layered silicates, carbon nanotubes, layered double hydroxides (LDH), graphitic carbon nitride and many more. Flame retardants that contain halogens, such as chlorine, bromine, fluorine, and iodine, have chemical groups in them. The usage of halogen-containing flame retardants is limited despite their good flame-retardant properties and lower cost because the type of fumes they produce varies depending on the type of flame retardant. Furthermore, when halogen-containing flame retardants burn, they produce a lot of smoke and poisonous or cancer-causing chemicals that could lead to dangerous situations [49]. Manufacturers are required to replace conventional halogenated flame retardants with new materials that have comparable properties by the new environmental rules. Consequently, within the past ten years, non-halogenated flame retardants have been an improved additive in engineering plastics. Low quantities of halogen-free flame retardants in polyurethane foams can lower the danger of hazard and fire. The benefits of non-halogenated flame retardants are their low toxicity and potent ability to stop the spread of fire. Moreover, polymers treated with nonhalogenated flame retardants can be reasonably priced, non-toxic, and ecologically beneficial while still meeting end-user criteria [50].

1.9. The Objective of this Research

This project aimed to create rigid polyurethane foams using a bio-based polyol and combine them with flame retardants to increase their fire resistance. To move away from traditional petroleum-based materials and explore renewable resources for polyol

synthesis. To develop flame-retardant solutions that are halogen-free and environmentally friendly. Here, soybean oil is converted into a polyol that is more reactive with isocyanate by epoxidation followed by ring opening. Before preparing the foams, confirmatory tests such as FT-IR, hydroxyl value, GPC, and similar ones were carried out to examine the creation of the bio-based polyol. MA, MC, and CMA are examples of non-halogenated flame retardants that were applied separately and in varying quantities to examine how they affected the foams' flammability and other characteristics. The investigation of soybean oil-based foams' shape, density, compression, thermal stability, and other significant characteristics was done.

CHAPTER II

MATERIALS AND METHODS

2.1. Materials

Soybean oil for the synthesis of SBO-polyol was procured from a local Walmart in Pittsburg, KS, USA. The chemicals and materials, including glacial acetic acid, hydrogen peroxide, toluene, amberlite IR120 H, sodium chloride, sodium sulfate, tetrafluoroboric acid, methanol, and lewatit MP 64, were purchased from Fischer Scientific in Allentown, PA, USA. For the synthesis of RPUFs, catalysts 1,4-diazabicyclo[2.2.2]octane (DABCO) and dibutylin dilaurate (DBTDL) were obtained from Air Products in Allentown, PA, USA. The silicon surfactant tegostab B-8404 was supplied by Evonik in Parsippany, NJ, USA. Huntsman in the Woodlands, TX, USA, provided jeffol SG-522 (Sucrose polyol with OH# 522) and rubinate M isocyanate (methylene diphenyl diisocyanate). Distilled water, used as a solvent and blowing agent, was purchased locally from Walmart, and HPLC-grade water was sourced from Fischer Scientific. Flame retardants, melamine and melamine cyanurate, were supplied by Sigma Aldrich in St. Louis, MO, USA, and 2-carboxyethyl(phenyl)phosphinic acid (CEPP) was obtained from TCI (Shanghai) Development Co., Ltd.

2.1.1. Soybean Oil

Soybean oil is a vegetable oil derived from soybean (Glycine max) seeds. Both unsaturated and saturated fatty acids are present in soybean oil triglycerides. Depending on the variety and harvest-related meteorological factors, the percentage of unsaturated fatty acids can surpass 80%. It is possible to insert functional groups into oil by using its unsaturated sites [51]. The primary objective for the creation of more reactive sites in the development of bio-based polyols in this work was the presence of the carbon-carbon double bond in the triglycerides depicted in the chemical structure of soybean oil (**Figure 5**). After the double bonds were broken and turned into an epoxide, methanol was added to cause a ring-opening reaction that produced a polyol. In addition, a commercially available polyol called jeffol 520 which is based on sucrose was also used to supplement the formulation whose hydroxyl number is 520 mg KOH/mg.

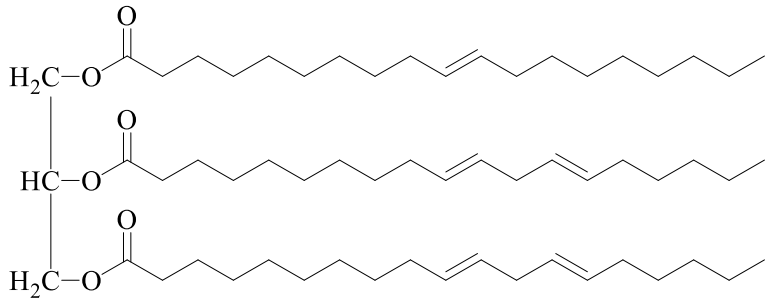

Figure 5. Soybean Oil.

2.1.2. Methylene Diphenyl Diisocyanate

Methylene diphenyl diisocyanate (MDI) has a lower vapor pressure and produces a more uniform reaction kinetics, so it is more widely utilized and less dangerous overall [52]. In this work, rigid polyurethane foam derived from biobased

sources is synthesized using Rubinate M isocyanate, or MDI. In **Figure 6**, the chemical structure of MDI is displayed. At room temperature, its viscosity was 0.21 Pa.s, its equivalent weight was 135 and its N=C=O content was around 31%.

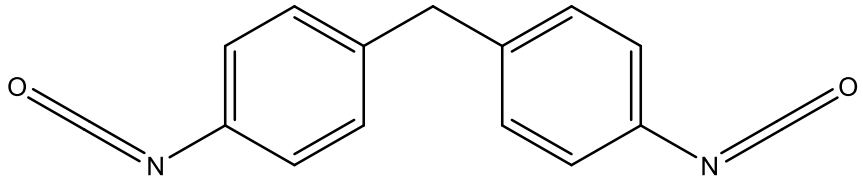

Figure 6. Methylene diphenyl diisocyanate.

2.1.3. Catalyst

For industries, catalysts are essential since they increase reaction rates and provide efficient curing procedures. Tertiary amine and organometallic-based catalysts are the two primary categories of catalysts that are frequently utilized. NIAX-A1 and T-12 were utilized for that, in that order.

2.1.4. Blowing Agent

Distilled water serves as the chosen blowing agent in this work due to its practicality, cost-effectiveness, and environmentally friendly characteristics. Its primary purpose is to regulate the cellular structure of polyurethane and control density. Water's involvement includes its reaction with isocyanate, leading to the formation of an unstable carbamic acid. This compound swiftly decomposes into a primary amine and CO_2, with the latter acting as the gas that induces the formation of the foamed and porous structure in the material.

2.1.5. Surfactant

Isocyanates and hydroxyl groups demonstrate a strong reactivity towards each other, but their tendency to form a heterogeneous phase arises from a lack of attractive intermolecular interactions. To counteract this, surfactants are utilized to create a stable dispersion, resulting in a uniform pore size in the foam. The introduction of surfactants also hinders the coalescence of bubbles during the foaming process, thereby shaping the porous structure of rigid foams. In this study, B-8404 surfactant was utilized for these specific purposes.

2.1.6. Flame-Retardants

In this experiment, three additives FR were investigated:

2.1.6.1. Melamine (MA)

The primary organic nitrogen compounds utilized as additive flame retardants are melamine and its derivatives. The stable white crystalline compound melamine (2, 4, 6-triamino-1, 3, 5 triazine) shown in **Figure 7** has a nitrogen content of 67%. Because of its stable structure and rich nitrogen, melamine is frequently utilized in polyurethane foams. This helps make RPUFs more fire-resistant and reduces smoke density during burning [53]. When melamine is heated, it can also produce gases that contain nitrogen, which will lessen the amount of combustible gases that are released when the matrix degrades. Melamine is an endothermic substance that creates condensed products such as melam, melem, and melon by absorbing heat and removing ammonia. Melamine also works as a flame dilution. The char layer that forms on these products gives them more

heat stability than pure melamine. With an increase in melamine content, mechanical characteristics like density and compression strength rise [54].

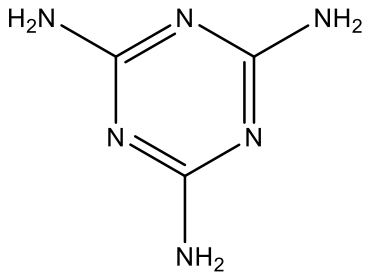

Figure 7. Structure of Melamine.

2.1.6.2. Melamine Cyanurate (MC)

Equimolar amounts of cyanuric acid and melamine were combined in an aqueous solution, and this mixture was evaporated to create melamine cyanurate, an organic crystalline complex. Melamine and cyanuric acid are linked by a specific 2D network structure of hydrogen bonds, as seen in **Figure 8**, which improves the thermal stability lowers the overall volatility of MC, and further forms an appropriate fire resistance for flammable polymers and other substrates. MC is very useful for enhancing the fire safety of nitrogen-based polymers, like thermoplastics (polyurethane) and polyamides (nylons) [55]. MC forms the condensation polymers melam, melem, and melom, which make up the superficial char layer, using endothermic breakdown that produces ammonia [56]. It breaks down to NH_3, CO_2, and H_2O at a high temperature after removing cyanuric acid and melamine [57].

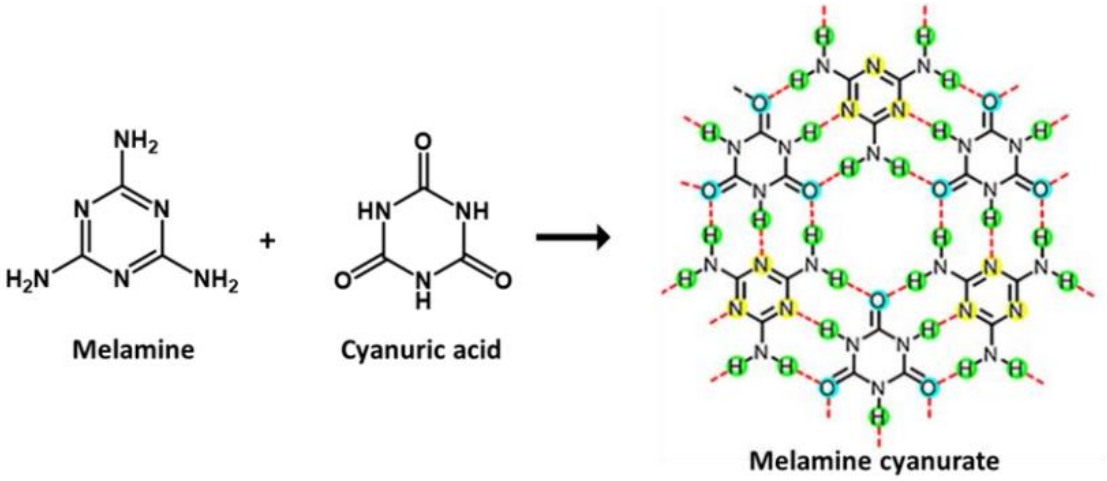

Figure 8. Structure of melamine cyanurate. Adapted with permission [57]. Copyright 2018, Elsevier.

2.1.6.3. 2-Carboxyethyl(phenyl)phosphinic Acid Melamine Salt (CMA)

The compound 2-carboxyethyl(phenyl)phosphinic acid is a phosphinic acid derivative with a carboxyethyl group and a phenyl group attached to the phosphorus atom. Phosphorus-containing compounds are often used as flame retardants because they can interfere with the combustion process. They can act by promoting char formation, inhibiting the release of flammable gases, and disrupting the combustion chain reactions. CMA was prepared by the reaction between 2-Carboxyethyl(phenyl)phosphinic acid (CEPP) and Melamine (MA). The nitrogen and phosphorus in CMA may work in concert to prevent char formation, which would increase PU's ability to withstand flames. In addition, at higher temperatures of decomposition, CMA can create phosphoric anhydrides or similar acids, which in turn encourage the development of char. Compared to carbonaceous char generated from PU without FR, this char with a phospho-carbonaceous structure was more stable [58].

2.2. Synthesis of CMA Flame-Retardant

In a 250 ml three-necked round-bottomed flask, 44 grams of 2-Carboxyethyl(phenyl)phosphinic acid (CEPP) was dissolved in 600 ml of deionized water and heated in an oil bath at 90°C. Subsequently, 25.90 grams of melamine was added to the solution, and the reaction proceeded for 6 hours. The resulting mixture became hazy, generating a white precipitate. Following this, the solution was promptly filtered, and the resultant white product was collected. The CMA product underwent vacuum drying until a constant weight was achieved. The synthesis of CMA is illustrated in **Figure 9**.

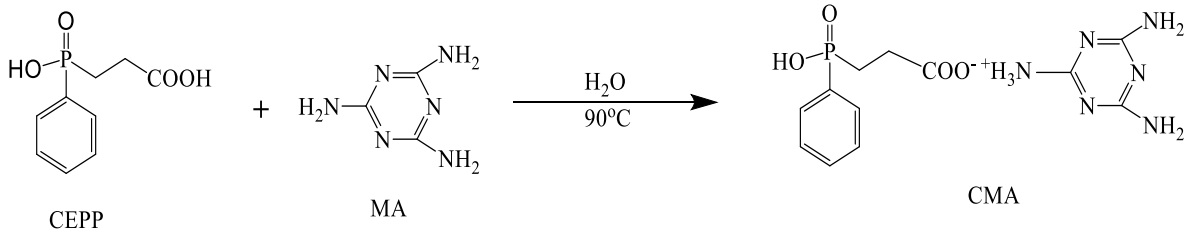

Figure 9. Synthesis of CMA.

2.3. Synthesis of Soybean Oil-Based Polyol

2.3.1. Epoxidation of Soybean Oil (SBO)

In this study, we followed a synthetic route like established methods for introducing epoxy groups into soybean oil by breaking unsaturation, a process involving the reaction of peroxy acids with double bonds [59], [60]. The experimental procedure took place in a 3-necked round-bottomed flask (1L): 300 grams of soybean oil, 150 ml of toluene, and 75 grams of Amberlite ion exchange resin were stirred mechanically in a water bath with an adjustable heating platform for 15 minutes at room temperature. After cooling the reaction to 5-10 °C with ice cubes, glacial acetic acid

(47.1 ml) was added dropwise, followed by 266.5 ml of 30% hydrogen peroxide. The mixture was continuously stirred for 7 hours at 70 °C. Once the reagents were completely added, the reaction mixture was cooled to room temperature, allowing the ion exchange resin to settle, and then filtered using a funnel. Further separation occurred using a separation funnel after multiple washes with a 10% Brine solution. Around 3 gm of sodium sulfate was added which acted as a drying agent, and the remaining solvents were removed from the epoxidized soybean oil (ESBO) through rotary evaporation.

2.3.2. Ring Opening of Epoxidized Soybean Oil into Polyol

Methanol was employed to catalyze the ring-opening of the epoxide, generating hydroxyl functional groups at a 7:1 mol ratio of methanol to the epoxide groups synthesized in ESBO. Tetrafluoroboric acid was utilized in a mixture consisting of 48 wt% water, 0.05% methanol, and ESBO. Methanol served as the nucleophile in this reaction, whereas tetrafluoroboric acid served as the catalyst. The reaction took place in a three-necked flask equipped with a condenser and a dropping funnel. Methanol (394.2 g) and tetrafluoroboric acid (0.8 g) were introduced to the flask and mechanically stirred at 70 °C. After a brief period of stirring and refluxing, ESBO was added dropwise, and the reaction was refluxed for one hour. Subsequently, the reaction mixture was cooled to room temperature to prevent hydrolysis while concurrently neutralizing it with the basic ion exchange resin Lewatit MP 64 (21.4 g) and stirred for 45 min. Following confirmation of a neutral mixture through a pH test, the resin was filtered out, and any excess solvents were eliminated through rotary evaporation. **Figure 10** illustrates the overall structural and bond changes occurring during the

synthesis of the polyol from soybean oil, involving both epoxidation and ring-opening reactions.

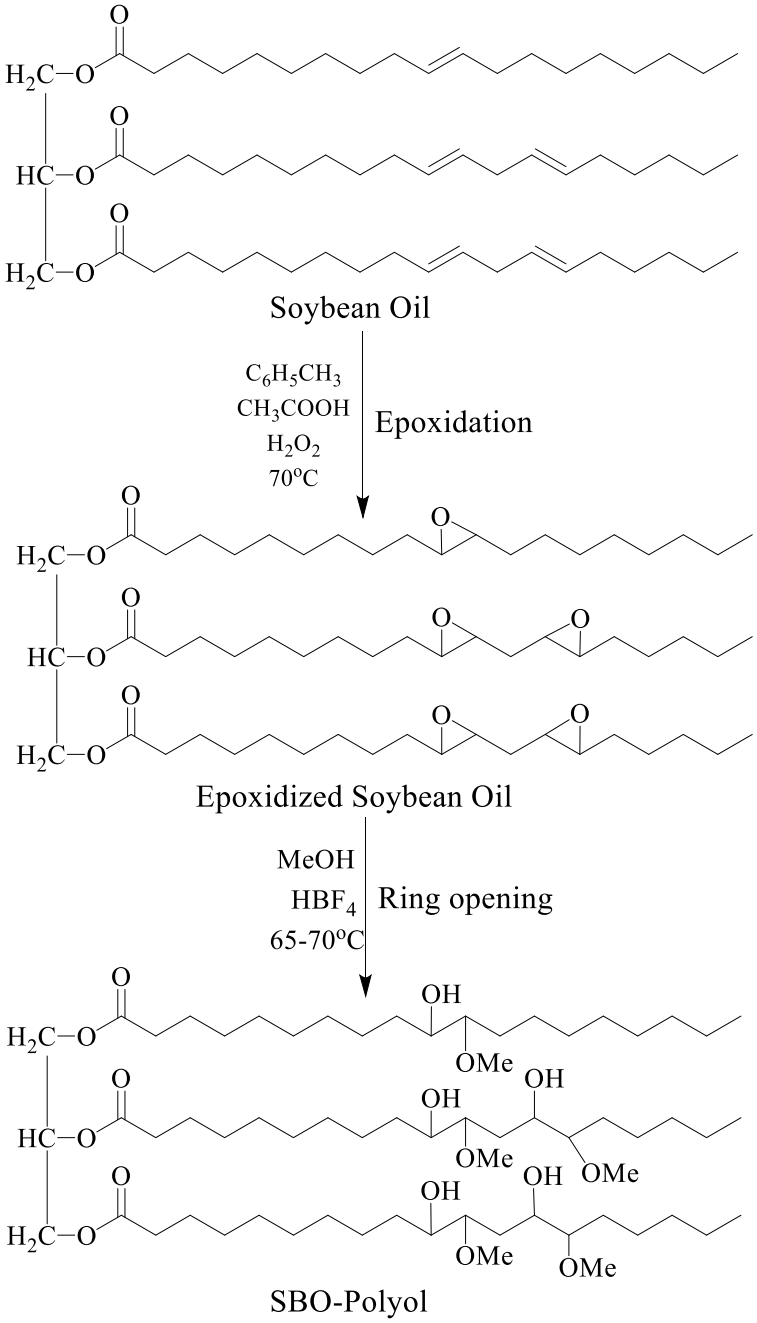

Figure 10. Synthesis of SBO-Polyol.

2.4. Characterization of Soybean Oil-Based Polyol

2.4.1. Iodine Value

The quantification of double bonds in the unsaturated compound was determined through the iodine value, a parameter reflecting the soybean oil's reactivity with iodine. A higher iodine value suggests increased unsaturation in the fatty acids [42]. In this experimental procedure, the number of double bonds in the soybean oil, utilized in polyol synthesis, was approximated using the Hanus method. A quantity of about 0.20 grams of soybean oil was mixed with 10 ml of chloroform ($CHCl_3$) in a 250-ml Erlenmeyer flask. Following this, 20 ml of Hanus reagent (BrI) was added to the solution, and after gentle shaking, the mixture was allowed to sit in the dark for an hour. Subsequent steps involved the addition of 20 ml of a 10% potassium iodide (KI) solution and 50 ml of HPLC-grade water to the flask, creating a uniform solution through stirring. Six drops of the starch indicator were introduced and the red solution was titrated with sodium thiosulphate ($Na_2S_2O_3$) until a clear solution (colorless) was achieved.

2.4.2. Epoxide Number

The epoxy oxygen content (EOC%) was determined using tetraethylammonium bromide and glacial acetic acid, providing a reliable method to assess the generation of epoxide groups from double bonds. In this procedure, epoxy soybean oil, weighing about 0.2 grams, was mixed into a 50 ml solution of tetraethylammonium bromide (TEAB) and stirred for 10 mins. The addition of a drop of crystal violet indicator preceded the titration of the solution using 0.1 N perchloric acid ($HClO_4$). The titration reached completion when the color transitioned from blue

to green. The recorded volume was then employed to quantify the epoxy content present in the epoxidized soybean oil.

2.4.3. Hydroxyl Value

The hydroxyl number, a pivotal parameter indicating a polyol's functionality and the requisite isocyanate quantity for an efficient chemical reaction, was determined for the soybean polyol using the phthalic anhydride pyridine (PAP) technique following ASTM-D 4274. In this process, 10 ml of a hydroxyl solution was added to 0.6 g of the synthesized soybean polyol within a glass bottle. The bottles, loosely capped, were placed at 100 °C in a preheated oven for 70 mins, with intermittent shaking every 15 minutes. Subsequently, the mixture was cooled to room temperature, followed by the addition of 10 ml of HPLC-grade water and 20 ml of isopropanol. After 10 minutes of agitation, 1 N potassium hydroxide (KOH) was incrementally introduced and titrated until a pink color emerged. The volume was recorded and utilized in the calculation of the hydroxyl number.

2.4.4. Acid Value

To ensure the optimal pH levels required for polyurethane foam synthesis, the acid value was measured at different stages throughout the polyol synthesis process, following the IUPAC 2.201 standard procedure. About 3 g of sample was dissolved in a 30 ml solvent mixture comprising isopropanol, toluene, and a phenolphthalein indicator. The solution was then titrated with 0.1 N potassium hydroxide (KOH) until a pink color change was observed. The recorded volume of potassium hydroxide used in the titration was employed to calculate the acid values.

2.4.5. Fourier-Transform Infrared Spectroscopy (FT-IR)

Fourier-transform infrared spectroscopy serves as a swift and effective method for identifying individual functional groups within a chemical compound. Unlike alternative tests, it eliminates the necessity for sample purification and operates without the need for solvents. The FTIR spectra of the samples were captured using a PerkinElmer Spectrum Two Spectrophotometer (**Figure 11**). The scans covered the spectral range of 4000-400 cm^{-1} with a resolution of 4 cm^{-1} and an averaging of 64 scans, contributing to the rapid and detailed analysis of the chemical composition.

Figure 11. Instrument for FT-IR analysis.

2.4.6. Viscosity

Viscosity, a key indicator of a substance's resistance to flow, can convey important information about its molecular weight-low viscosity suggests a lower molecular weight, while high viscosity may indicate a larger molecular weight. Furthermore, low viscosity is often associated with improved processability. In the

specific context of this experiment, the ease of polyurethane synthesis is anticipated to be impacted by the viscosity of the SBO polyol. Additionally, the viscosity parameter plays a crucial role in confirming the accurate production of the polyol using soybean epoxide. The analysis employed an AR 2000 dynamic stress rheometer from TA Instruments, USA, as depicted in **Figure 12**. Viscosity measurements were conducted at 25 °C, with shear stress systematically increasing from 1 to 2000 Pa linearly. The dynamic rheometer was equipped with a cone plate featuring an angle of 2° and a cone diameter of 25 mm.

Figure 12: AR 2000 dynamic stress rheometer for measuring viscosity.

2.4.7. Gel Permeation Chromatography (GPC)

In this size exclusion method, molecules are separated based on their excluded volume, which is directly associated with molecular weight. Following the processes of epoxidation and ring-opening reactions, the soybean epoxide and polyol derived

from the oil were examined and confirmed using this characterization technique. The project utilized the Waters GPC instrument from Milford, MA, USA, as illustrated in **Figure 13**. The instrument facilitates the separation of molecules with different molecular weights by employing a range of pore diameters. The GPC instrument comprised four Phenogel columns measuring 300 × 7.8 mm, each with distinct pore sizes: 50, 102, 103, and 104 Å. Tetrahydrofuran (THF) was chosen as the eluent solvent, maintaining a consistent eluent rate of 1 ml/min at 30 °C. This setup ensured effective separation and analysis of the components of interest.

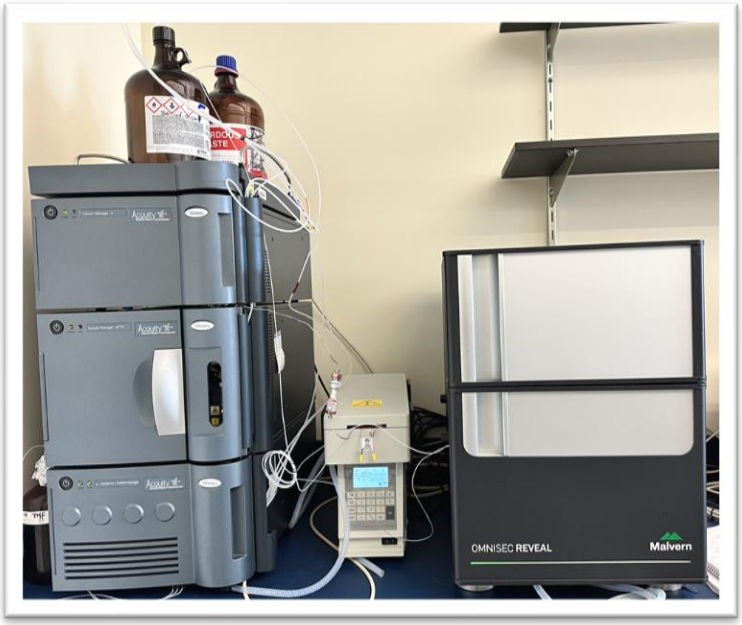

Figure 13: GPC instrumental setup.

2.5. Preparation of Rigid Polyurethane Foam (RPUF)

Following the confirmation of the production of soybean oil-based polyol from pure soybean oil, the polyol was added to the rigid polyurethane foam formulation. Bio-based RPUFs were produced through a one-shot free-forming process, combining polyol and isocyanate with a catalyst, surfactant, blowing agent, and flame-retardant

additive. During the preparation of RPUF based on soybean oil-derived polyol, three sets of foams were created with varying concentrations of non-halogenated flame retardants such as melamine (MA), melamine cyanurate (MC), or 2-carboxyethyl(phenyl)phosphinic acid melamine salt (CMA). These foams had identical ingredient proportions as outlined in **Tables 1, 2,** and **3**. In a plastic cup, a commercial polyol (SG-522) was blended in a 1:1 ratio with the specified SBO-polyol in the formulation. The mixing process involved stirring SBO-polyol, SG-522, A-1, T12, B8404, water, and increasing concentrations of MA, MC, and CMA in respective formulations using a high-speed mechanical stirrer to achieve a homogeneous mixture. Subsequently, an equal molar ratio of isocyanate was added slowly and immediately stirred vigorously for a brief period, allowing the foam to expand at room temperature. The foams were then left to cure completely at room temperature for approximately one week before undergoing further characterization.

Table 1. SBO-RPUF Formulation with MA. All numbers are in grams except Wt % of MA.

Ingredients	MA-0	MA-1	MA-2	MA-5	MA-7	MA-10	MA-12	MA-15
SBO-Polyol	10	10	10	10	10	10	10	10
SG-522	10	10	10	10	10	10	10	10
A-1	0.18	0.18	0.18	0.18	0.18	0.18	0.18	0.18
Water	0.8	0.8	0.8	0.8	0.8	0.8	0.8	0.8
T-12	0.04	0.04	0.04	0.04	0.04	0.04	0.04	0.04
B8404	0.4	0.4	0.4	0.4	0.4	0.4	0.4	0.4
Isocyanate	31.1	31.1	31.1	31.1	31.1	31.1	31.1	31.1
MA	0	1	2	5	7	10	12	15
Wt % of MA	0	1.9	3.81	9.52	13.33	19.04	22.85	28.56

Table 2. SBO-RPUF Formulation with MC. All numbers are in grams except Wt % of MC.

Ingredients	MC-0	MC-1	MC-2	MC-3	MC-4	MC-5	MC-6	MC-7
SBO-Polyol	10	10	10	10	10	10	10	10
SG-522	10	10	10	10	10	10	10	10
A-1	0.18	0.18	0.18	0.18	0.18	0.18	0.18	0.18
Water	0.8	0.8	0.8	0.8	0.8	0.8	0.8	0.8
T-12	0.04	0.04	0.04	0.04	0.04	0.04	0.04	0.04
B8404	0.4	0.4	0.4	0.4	0.4	0.4	0.4	0.4
Isocyanate	31.1	31.1	31.1	31.1	31.1	31.1	31.1	31.1
MC	0	1	2	5	7	10	12	15
Wt % of MC	0	1.9	3.81	9.52	13.33	19.04	22.85	28.56

Table 3. SBO-RPUF Formulation with CMA. All numbers are in grams except Wt % of CMA.

Ingredients	CMA-0	CMA-1	CMA-2	CMA-3	CMA-4	CMA-5	CMA-6	CMA-7
SBO-Polyol	10	10	10	10	10	10	10	10
SG-522	10	10	10	10	10	10	10	10
A-1	0.18	0.18	0.18	0.18	0.18	0.18	0.18	0.18
Water	0.8	0.8	0.8	0.8	0.8	0.8	0.8	0.8
T-12	0.04	0.04	0.04	0.04	0.04	0.04	0.04	0.04
B8404	0.4	0.4	0.4	0.4	0.4	0.4	0.4	0.4
Isocyanate	31.1	31.1	31.1	31.1	31.1	31.1	31.1	31.1
CMA	0	1	2	5	7	10	12	15
Wt % of CMA	0	1.9	3.81	9.52	13.33	19.04	22.85	28.56

2.6. Characterization of the Bio-Based Foams

Following a week, the foams underwent cutting into standardized sizes and shapes by using a table saw. Further examinations with detailed descriptions are provided below.

2.6.1. Apparent Density

Density is a crucial factor that impacts the physicomechanical properties and overall performance of the foam. The apparent density, obtained by dividing mass by

volume, is a key metric in this regard. The density of foam is influenced by the internal volume of pores distributed throughout the cross-linked matrix. In this study, foams were shaped into cylinders with dimensions of 45 × 30 mm (diameter × height) to calculate density according to the ASTM D1622 standard.

2.6.2. Closed Cell Content (CCC)

Foam classification relies on the cell structure, categorized as either open or closed-cell. To ascertain the distribution of closed or open cells in soybean oil-based flame retardant foams, the closed cell content was measured. Utilizing the Ultrafoam 1000 ultrapycnometer, as depicted in **Figure 14**, the measurement followed the ASTM D2856 standard. This instrument comprises two interconnected sections: a chamber and a pressure-temperature sensor. The process involved measuring the volume of the empty chamber by introducing nitrogen gas through the valve. Following this, a cylindrical sample with known dimensions and mass was placed into the chamber to determine the closed-cell content.

Figure 14: Ultrapycnometer (Ultrafoam 1000).

2.6.3. Compressive Strength Test

Compressive strength, defined as the maximum force applied over a material's surface, was assessed through the compression of foam between parallel plates using a gradually applied load. The analysis utilized the "Q test 2-tensile machine," a universal electronic tensile tester, following the ASTM D 1621 standard (**Figure 15**). For the preparation of samples, polyurethane foams were shaped into cylindrical forms with dimensions of 45 × 30 mm (diameter × height). These foam samples were then placed between two parallel compression plates on a larger surface. The compressive strength measurement was performed at 10% strain using Blue Hill software, with a strain rate of 3 cm/min applied from the top.

Figure 15: Q test 2-tensile machine.

2.6.4. Scanning Electron Microscope (SEM) Imaging

Scanning electron microscopy was utilized to capture surface images by directing a beam of electrons onto the sample. The sample underwent exposure to a high-energy electron beam or ionized atoms, leading to the release of electrons from the surface. The interaction between the electron beam and the sample produced distinct signals, resulting in the final image. SEM revealed that the morphological structure provided vital information about the surface of the specimen. To obtain images of the foam samples, a two-step process was employed. Initially, the top section of the foam was cut into cubic shapes with dimensions of 0.5 cm for each side. These samples were then placed into a magnetron sputtering instrument for a thin coating of gold on their surfaces. The gold sputtering instrument, illustrated in **Figure 16** (Kurt J. Lesker Company), was crucial and applied before capturing images to enhance the specimen's

surface conductivity. In the second step, once the top of the polyurethane foam samples was coated with a thin conductive gold layer, images were captured using a Thermo Scientific Phenom Pure desktop SEM, sourced from the Sioux company in the Netherlands.

Figure 16. Gold layer sputtering (left), thermo scientific phenom (right).

2.6.5. Horizontal Burning Test

The properties of rigid polyurethane foams in the horizontal burning test were determined according to ASTM D4986-98. Rectangular specimens, measuring 150 mm in length, 50 mm in width, and 12.5 mm in thickness, were prepared. The weight of each sample was recorded, and subsequently, each foam specimen underwent a 10-second exposure to a direct flame. Measurements of self-extinguishing time and weight loss were taken after the exposure. This testing was conducted in a fume hood with strong ventilation to eliminate vapors generated during decomposition, as depicted in **Figure 17**.

Figure 17: Horizontal burning test under the fume hood.

2.6.6. Thermogravimetric Analysis (TGA)

Thermogravimetric analysis is a method for evaluating the thermal stability of materials by subjecting them to a consistent heating rate and monitoring the weight change of the sample with temperature. The TA instrument (TGA Q-500), illustrated in **Figure 18**, was used to study the thermal behavior and decomposition of rigid polyurethane foams. A sample of approximately 3-5 mg was placed on an aluminum pan and heated at a ramp rate of 10 °C/min, with the temperature reaching up to 600 °C under either a nitrogen or air atmosphere.

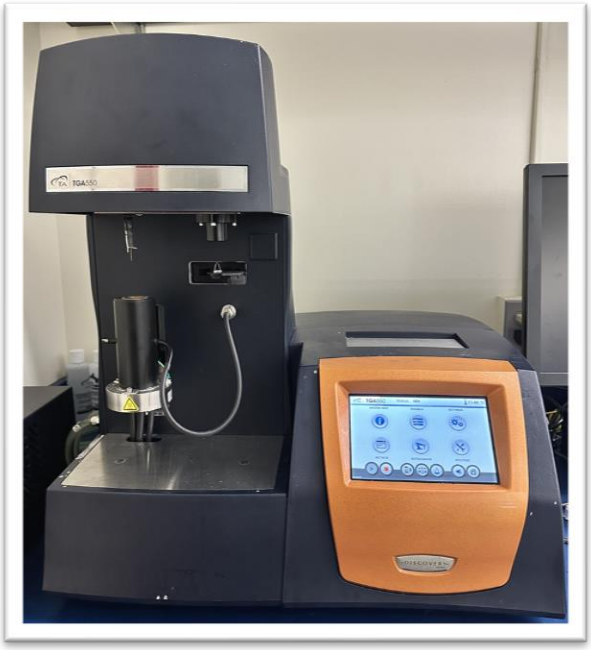

Figure 18: Thermogravimetric analysis instrument.

CHAPTER III

RESULTS AND DISCUSSIONS

In place of petroleum-based polyols, the bio-based polyol that was produced was utilized to make rigid polyurethane foams. Several experiments were conducted to verify the bio-based polyol's successful synthesis as well as to look into the rigid polyurethane foams' physicomechanical and thermal stability.

3.1. Properties of SBO, Epoxide and Polyol

3.1.1. Iodine Value

The amount of unsaturation or double bonds in soybean oil and its derivatives was ascertained by measuring the iodine value using the Hanus method. With an iodine value of 132.74 g I_2/100 g of oil, there were 0.52 moles of double bonds in every 100 g of purchased SBO. Stoichiometric calculations were used to establish the amount of reagents needed for the epoxidation reaction based on this result. The measured iodine values for the epoxide and polyol after the epoxidation and ring opening reactions were 5.04 g I_2/ 100 g and 1.63 g I_2/ 100 g, respectively. This indicates that the double bonds in SBO were changed into a more reactive and practical form for rigid polyurethane foams.

3.1.2. Epoxide Number

The quantity of epoxide groups in a substance is indicated by the percent oxirane number. Following the epoxidation reaction of the SBO with hydrogen peroxide and acetic acid in the presence of the catalyst, the epoxide number in this work was 7.21%. Following the ring-opening procedure, the epoxy concentration in the SBO polyol was detected to be around 0.06%, showing that the epoxide ring had been converted into hydroxyl groups.

3.1.3. Hydroxyl Value

The hydroxyl number is one of the most crucial characteristics of polyols since it establishes the reactivity and isocyanate content required to produce polyurethanes. The SBO polyol in this experiment had an OH number of 270.41 mg KOH/g. This amount served as the basis for calculating the amount of MDI needed to synthesize the rigid polyurethane foams.

3.1.4. Acid Value

An amine-based catalyst was employed to create the polyurethane foams derived from soybean oil. As a result, a very high acid value for the SBO polyol will prevent foaming since the acidic polyol and amine-based catalysts will not react as intended. Following SBO polyol production, an acid value of 0.93 mg KOH/g was established, whereas SBO and ESBO had 0.55 and 0.71 mg KOH/g respectively. This low number has very little impact on the catalysis involved in the synthesis of polyurethane foam.

3.1.5. Viscosity Measurement

The measurement of a material's resistance to flow is called viscosity, and it can have a big impact on how processable samples are. The measured viscosity of the SBO was 0.05 Pa.s, that of the epoxide SBO was 0.24 Pa.s, and that of the SBO polyol was 1.63 Pa.s. When the viscosity of the polyol gradually increases from SBO, it suggests that the molecular weights have increased during the transformation reactions. In contrast to other polyols, SBO polyol's low viscosity contributed to the foams' ease of processing [24].

3.1.6. Fourier-Transform Infrared Spectroscopy

The presence of several chemical bonds in a molecule can be determined using Fourier spectroscopy. This method was one of the easiest ways to verify that the polyol and epoxide from the SBO were synthesized. One common indicator of unsaturation in the FT-IR spectra of various fats and vegetable oils is observed at 2989–3029 cm^{-1} [61]. **Figure 19**'s infrared absorption spectrum shows the presence of a peak near the wavelength at 3010 cm^{-1}. Based on the stretching vibration from the =C-H linked to it, this peak indicates the presence of the carbon-carbon double bond in the SBO [62], [63]. But following the epoxidation process, this peak vanishes and a new one emerges at about 822 cm^{-1}. The bending originating from the epoxy group in the C-O-C ring is linked to this current peak. A broad peak that occurs at 3458 cm^{-1} serves as evidence of the SBO polyol. This wide peak is indicative of the stretching vibration that occurs when hydroxyl groups are present in a molecule [64], [65]. This confirms, among other experiments, the synthesis of polyol derived from SBO and its appropriateness for use in the production of rigid polyurethane foams.

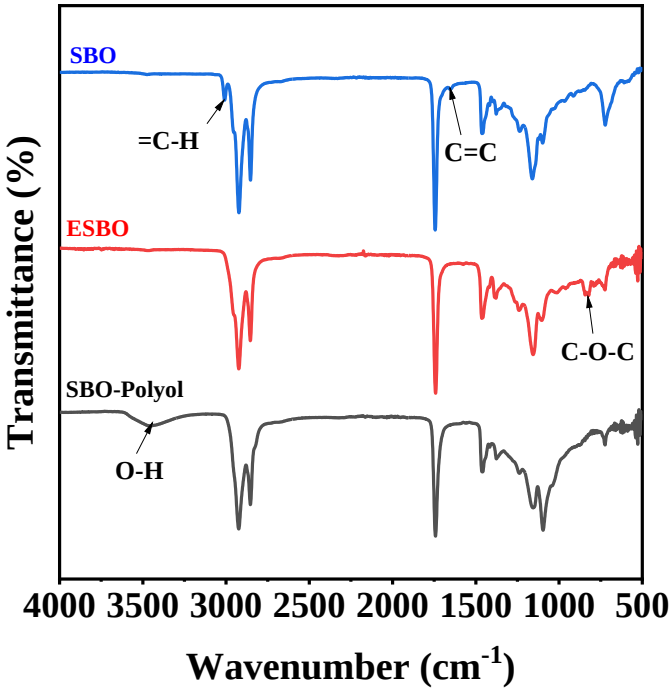

Figure 19: FTIR spectra of Soybean oil (SBO), Epoxidized soybean oil (ESBO) and SBO-Polyol.

3.1.7. Gel Permeation Chromatography

This is an analytical technique that can be used to track a reaction's development. Analytes can be divided based on the range of weights for a particular GPC column. Smaller molecules can more readily enter the pores in the column, stay in the column longer, and have a longer retention time because of the porous beads in the column. On the other hand, larger molecules will be easier to elute, require fewer pores to enter, and spend less time in the column. The SBO polyol emerges first at 32.06 minutes, as seen in **Figure 20**. The SBO and epoxide have respective retention times of 32.08 and 32.31 minutes.

When compared to the beginning and intermediate products, the SBO polyol's retention time was shorter, which suggests that the polyol's molecular weight and polymerization have increased. Around 30 minutes, a minor peak related to the SBO polyol is seen. This peak may be the consequence of a small amount of the polyol oligomerizing during the conversion process, as well as the creation of dimers and trimers due to the fluctuation in the fatty acids present [66]. While ESBO is polar, and SBO is non-polar. The polar character of the silica gel that is added to the GPC column may have reacted with ESBO (polar-polar interaction), causing the elution of ESBO to occur slowly.

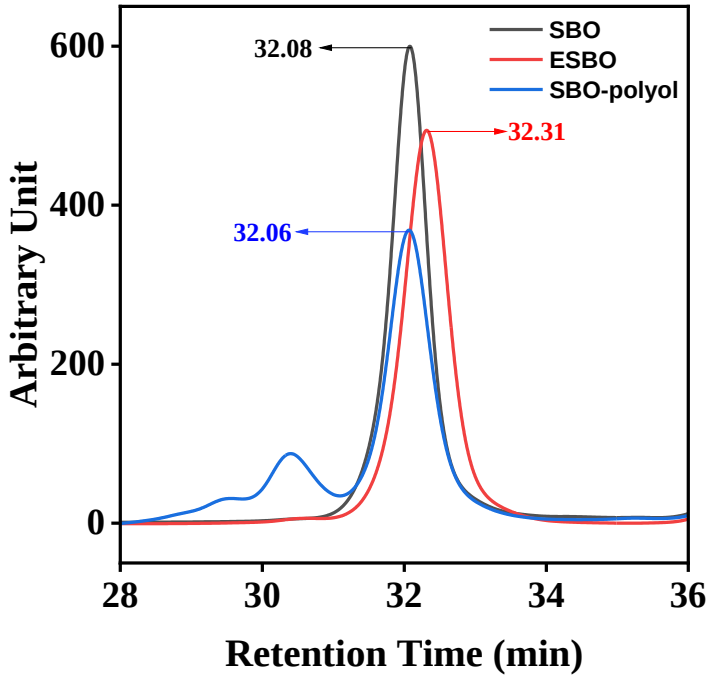

Figure 20: GPC of Soybean oil (SBO), Epoxidized soybean oil (ESBO) and SBO-Polyol.

3.2. Properties of Flame-Retardant

3.2.1. FT-IR of CMA

By using FT-IR, the chemical structure of CMA was verified. **Figure 21** displayed CEPP, MA, and CMA's FT-IR spectra. At 3466, and 3412 cm^{-1}, respectively, two vibration absorption maxima of primary amine in the 3000–3500 cm^{-1} range were detected [67]. In CEPP, a -C=O vibration absorption peak was at 1725 cm^{-1}, -C-O at 1440 $cm^{-1,}$ and -OH at 934 cm^{-1} was found [68], [69]. CMA showed two absorption peaks at 3361 and 3123 cm^{-1} because of the vibrational absorption of $-NH_2$ and $-NH_3^+$ [70], [71]. At 1507 cm^{-1}, another $-NH_3^+$ absorption peak was seen. The stretching vibration absorption of -C=O in CEPP, which was first detected at 1725 cm^{-1}, has shifted to 1648 cm^{-1} because of the synthesis of $-COO^-$ in CMA. The melamine salt was created when NH_2 and COOH were mixed, as shown by the presence of NH_3^+ and COO^- in CMA. Furthermore, the P(=O)-OH of CEPP showed a broad and mild absorption at 2555 cm^{-1}, but in CMA, this changed to 2507 cm^{-1} [70], [72]. This shift may have been caused by the steric and inductive action that results from the synthesis of melamine salt between the $-NH_2$ of melamine and the -COOH of CEPP.

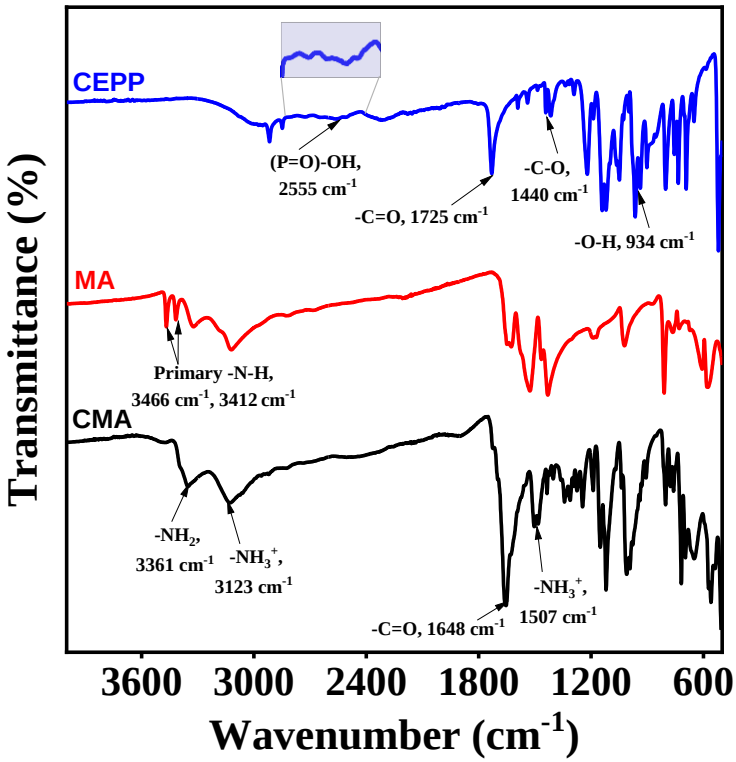

Figure 21: FT-IR of CEPP, MA, and CMA.

3.2.2. Thermal Degradation of FRs

Figure 22 depicts the heat deterioration of flame retardants. Gradual endothermic condensation is a recognized process for melamine that occurs during heating, producing compounds such as melam, melem, and melon, as well as ammonia, a flame diluent. These materials form the char layer because they are more heat-resistant than melamine. High temperatures are needed to create melons and melem. Graphitic carbon, or g-C_3N_4, is the product of the following heats [20], [73], [74]. Ammonia is the main volatile product that is produced in the first phase and is also evolved with some HCN [75]. The thermal degradation of melamine cyanurate may result in the

thermal breakdown of cyanuric acid and melamine. During deterioration, ammonia separates from melamine cyanurate, and cyanuric rings progressively bind together through imide bridges. The release of water and ammonia molecules, followed by the conversion of cyanuric acid into volatile cyanates, accounts for its weight loss. Amine groups replace carbonyl groups in cyanuric acid [55]. Thus, the flame retardancy of MC-filled PUF is attributed to the endothermic decomposition of melamine cyanurate (MC), which yields ammonia (a non-combustible gas) and condensation products such as melam, melem, and melom, which comprise the char layer [20].

It was observed that the 2-carboxyethyl(phenyl)phosphinic acid melamine salt (CMA) decomposes in four steps. The first maximum weight loss temperature was brought about by the removal of adsorbed water. The P–C bond breaking was the reason behind CMA's second-greatest weight loss temperature. The creation of polyphosphoric acid was responsible for the fourth-greatest weight loss, while the breakage of the ionic bond between COO^- and RNH_3^+ and the subsequent formation of cross-linked 2-carboxyethyl-(phenyl)phosphinic acid were the causes of the third maximum weight loss temperature [58], [76].

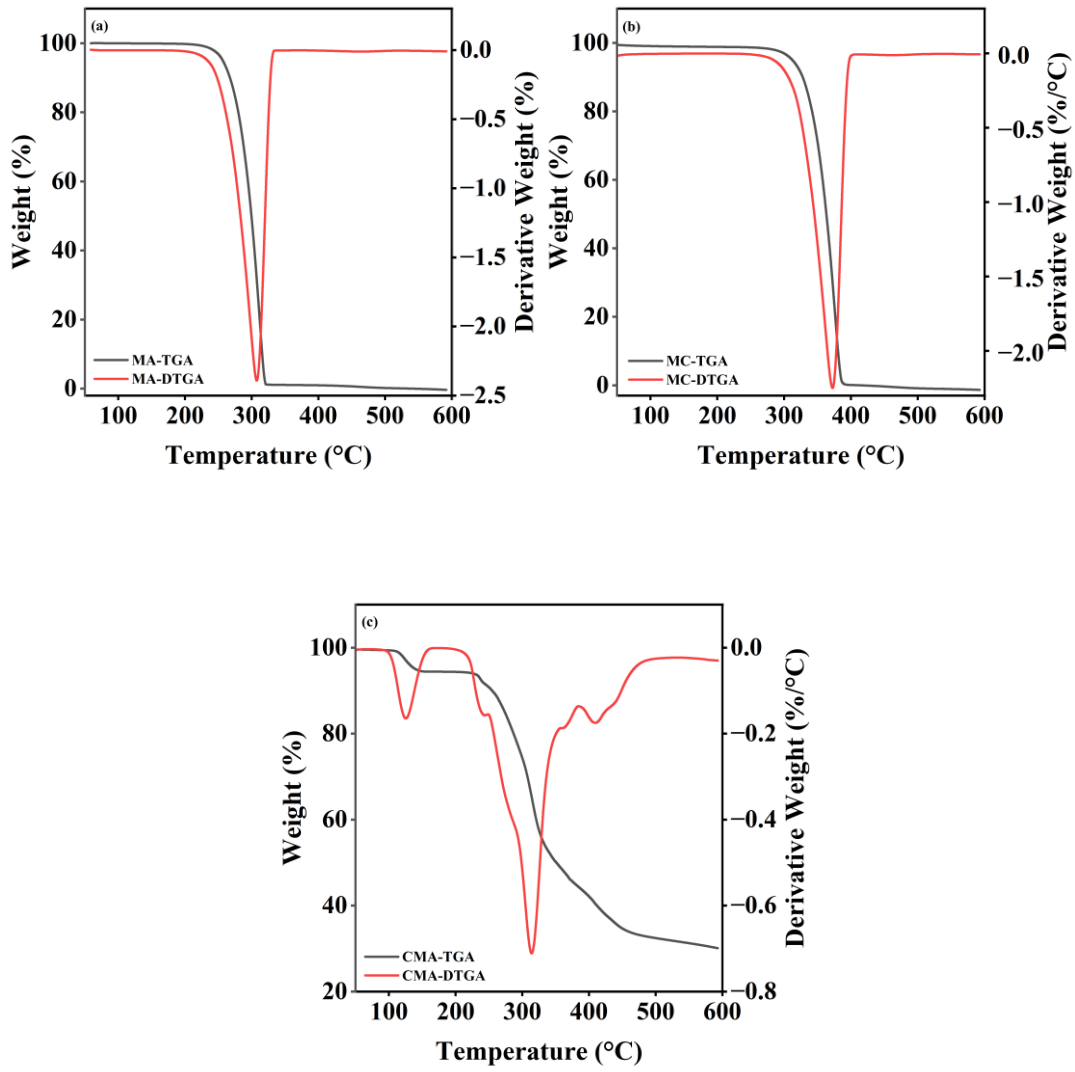

Figure 22. Thermal stability of flame retardants in a nitrogen atmosphere: TGA and DTGA [(a) MA, (b) MC, (c) CMA].

3.3. Properties of the SBO-Based Rigid Foams

Rigid polyurethane foams with various concentrations of flame retardants were created once the appropriate qualities of SBO polyol were established. Physically, the foams made from soybean oil were like those made commercially. The foams were standardized and cut to the required sizes, and their varied properties were examined.

Cell morphology, apparent density, closed cell content, mechanical properties, thermal stability, and flame retardancy are a few examples. For the characterization, the SBO polyurethane foam samples [without FR and with FR (MA, MC, and CMA - 1 gm and 12 gm)] were cut and taken from the inner zone of the foam into uniform sizes using a table saw, which was separated into three layers: the top (T), middle (M), and bottom (B) layers for better evaluation.

3.3.1. Cell Morphology

The primary objective of the study is to elucidate the physical characteristics of foams by scrutinizing their microstructure and morphology. **Figures 23, 24,** and **25** exhibit scanning electron microscopy (SEM) images of rigid polyurethane foam (RPUF) with increasing concentrations of MA, MC, and CMA. **Figures 26, 27, 28,** and **29** show the SEM images of the top, middle, and bottom portions of the foam. It is widely acknowledged that the mechanical properties of RPUF are notably affected by the cell structure of the foam. The pure foams exhibit circular and evenly dispersed cell sizes. Notably, foams containing MA and MC display a relatively uniform cell distribution with a mild increase in cell size. However, higher concentrations of MA and MC result in foams with a coarser morphology, leading to partial disruption of cell structures. Conversely, increasing the amount of CMA results in larger cell sizes and distortions, particularly beyond CMA-7 (13.33 wt % CMA), potentially causing the collapse of cellular structures. CMA is recognized to exist in the foam as hard particles, and its presence leads to foam shrinkage or cracking at higher concentrations. Furthermore, a higher concentration of CMA causes the aggregation of CMA particles,

contributing to the rupture and collapse of cellular structures. The average cell size is quantified using ASTM and Intercept methods and values are found to be as shown in **Table 3**.

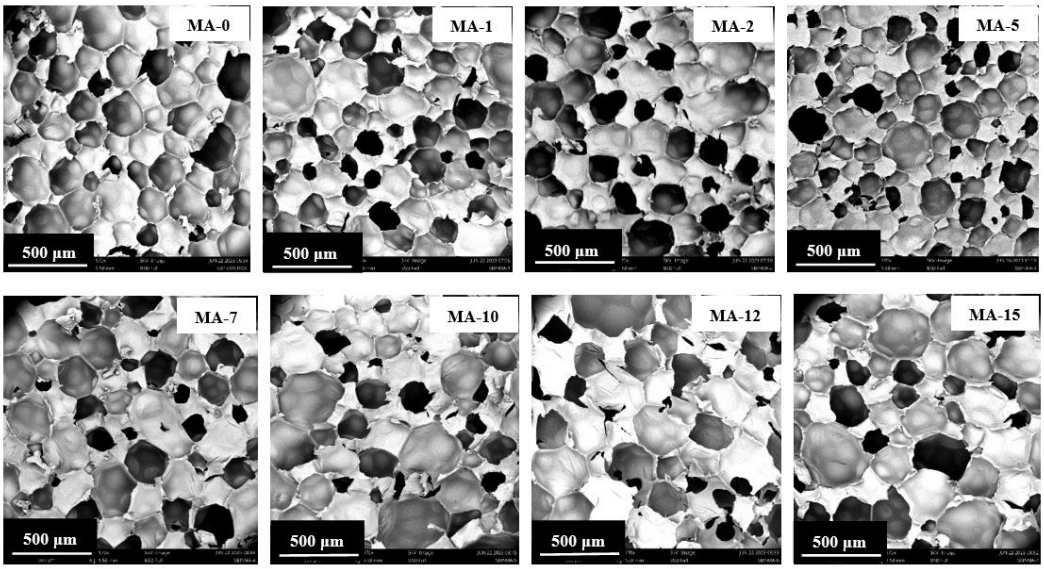

Figure 23. SEM images for SBO-based foams with varying amounts of MA.

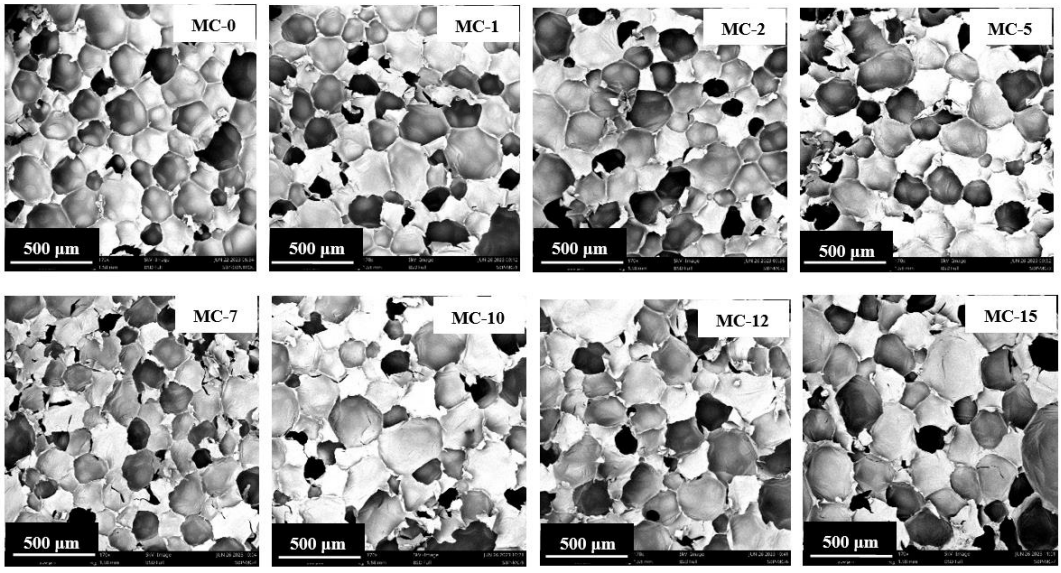

Figure 24. SEM images for SBO-based foams with varying amounts of MC.

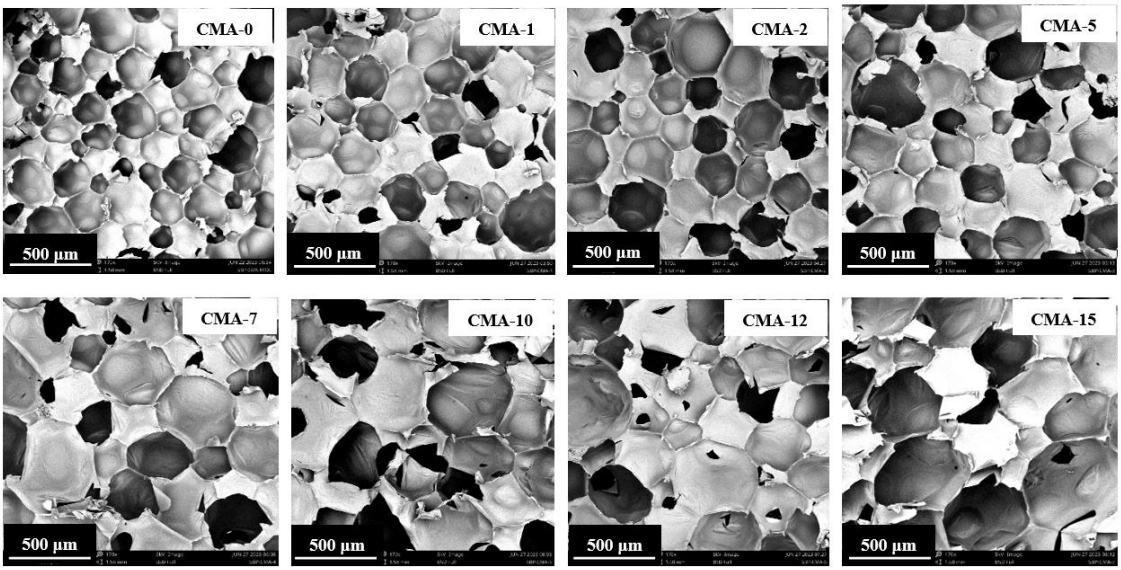

Figure 25. SEM images for SBO-based foams with varying amounts of CMA.

Table 4: Average cell size of SBO-based foams with varying amounts of FRs.

Sample	Cell Size (µm)		
FR weight (gm)	MA	MC	CMA
0	173	173	173
1	163	168	198
2	176	176	202
5	160	182	202
7	182	183	260
10	188	202	266
12	191	202	273
15	195	210	312

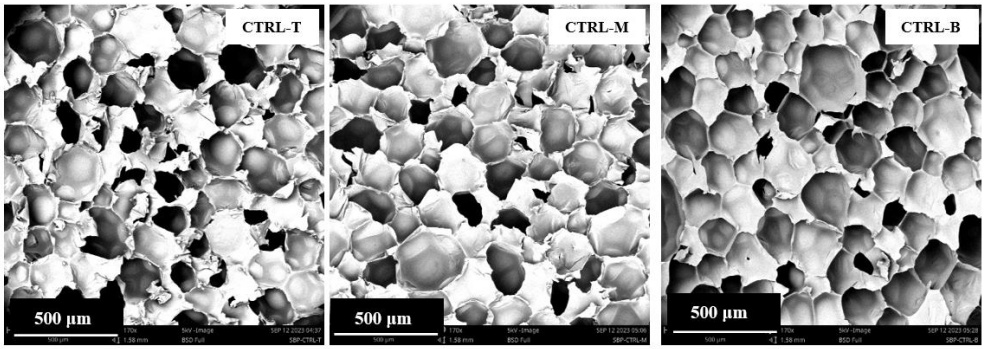

Figure 26. SEM images for SBO-based foams without FR.

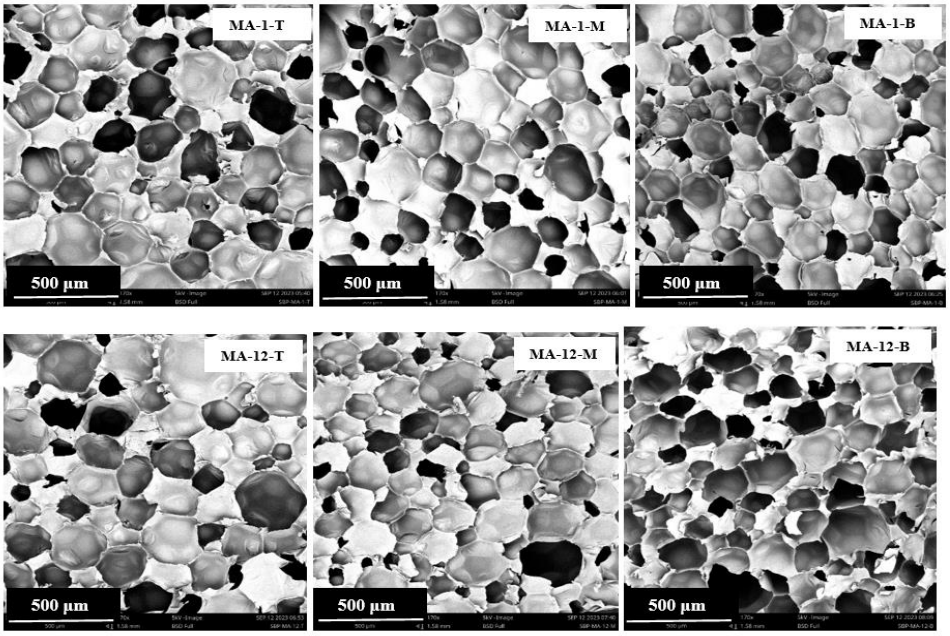

Figure 27. SEM images for SBO-based foams with MA-1 and MA-12 (Top, Middle, and Bottom).

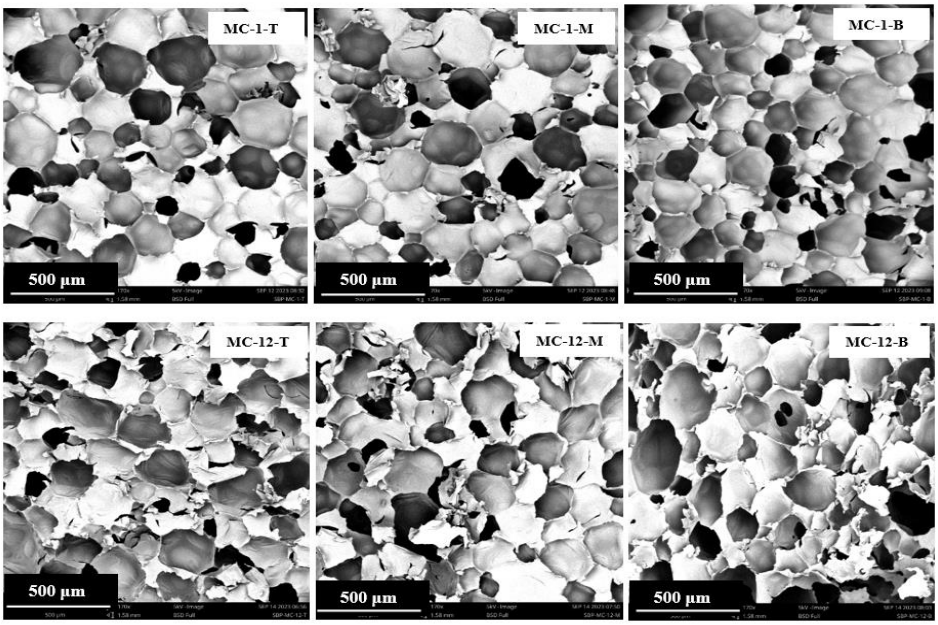

Figure 28. SEM images for SBO-based foams with MC-1 and MC-12 (Top, Middle, and Bottom).

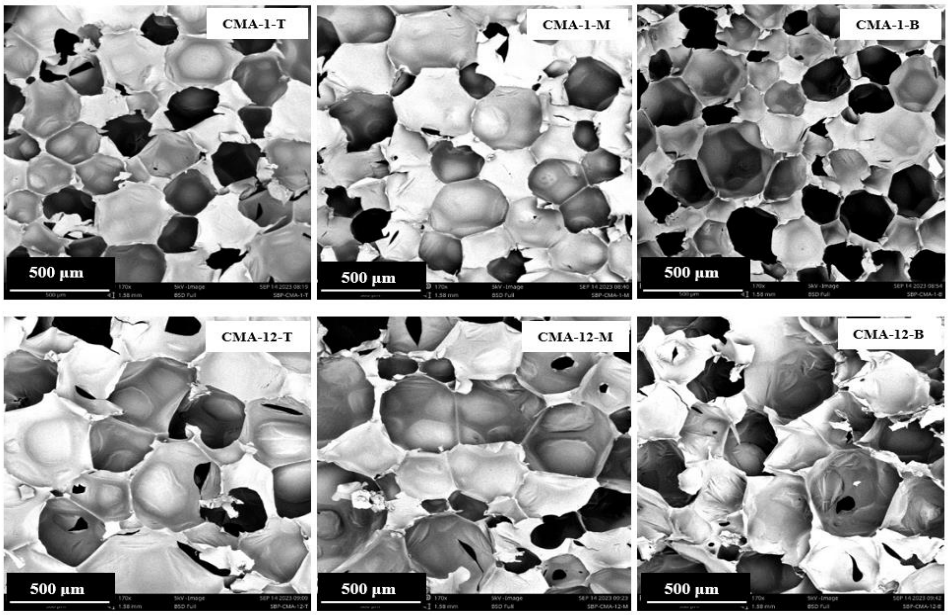

Figure 29. SEM images for SBO-based foams with CMA-1 and CMA-12 (Top, Middle, and Bottom).

3.3.2. Apparent Density

To examine how SBO-polyol and flame retardant (FR) impact the overall composition of biobased rigid polyurethane foam (RPUF), a thorough analysis of its physical properties was undertaken. Apparent density, a crucial factor for the foam's physical and mechanical characteristics, depends on crosslink density, cell morphology, and various other factors [77]. Typically, conventional RPUFs for specific applications exhibit densities ranging from 20 to 50 kg/m^3 without negatively affecting their cellular structures [78], [79]. The concentration of the blowing agent, a factor influencing foam density, was kept constant in this study, using HPLC-grade water as the blowing agent.

Figure 30 illustrates the apparent density of polyurethane foams derived from SBO-polyol. The inclusion of MA in RPUF resulted in apparent densities ranging from 31 to 47 kg/m^3, while MC and CMA exhibited densities of 31-44 kg/m^3 and 28-31 kg/m^3, respectively. A slight increase in foam density was observed with increasing amounts of MA and MC, likely due to the increased presence of MA and MC particles embedded in the cell structure. Conversely, after incorporating CMA, the density decreased with rising CMA concentration up to CMA-10 (19.04 wt % CMA). This phenomenon could be explained by SEM micrographs indicating a reduction in cell number due to an increase in cell size. The lack of interaction between CMA and the polyurethane matrix, leading to some degree of microphase separation, likely contributed to the density decrease [80][81].

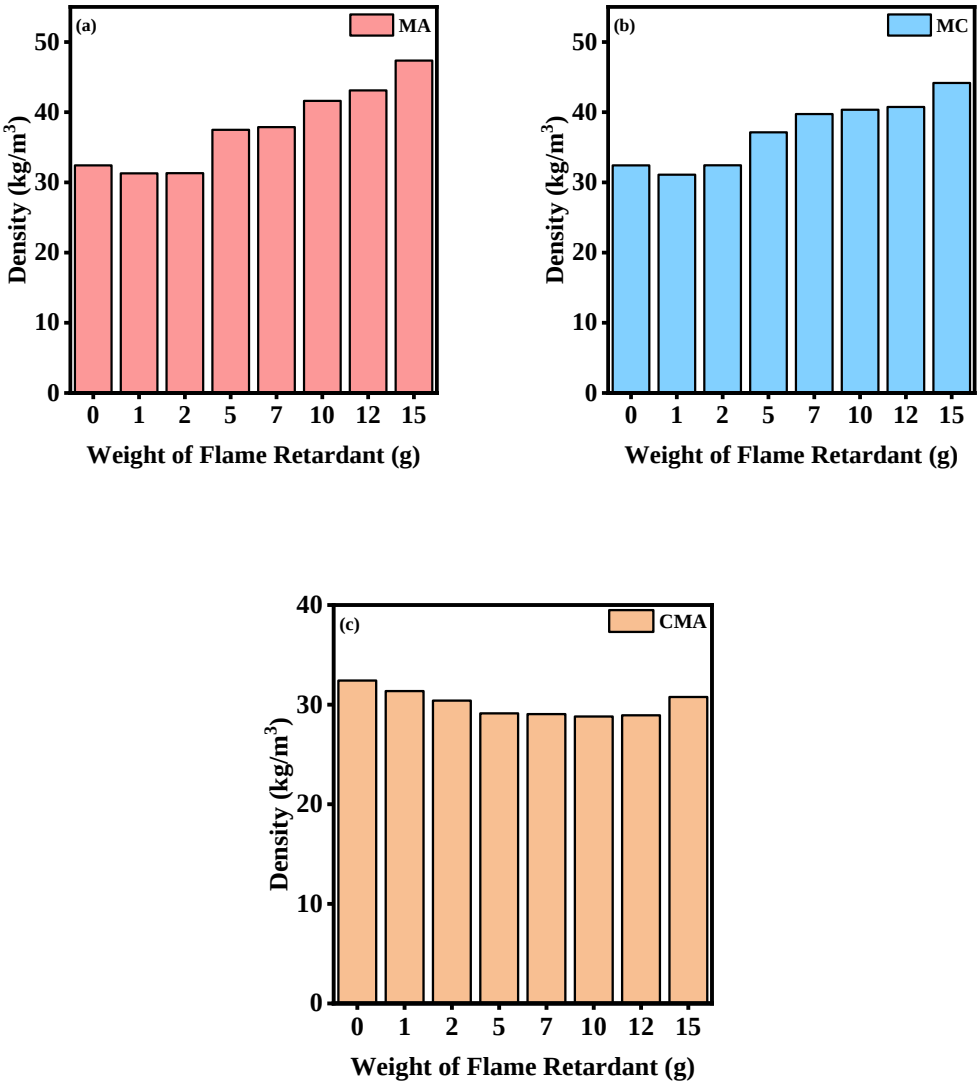

Figure 30: Apparent density of the obtained rigid PU foams with different weights of (a) MA, (b) MC, and (c) CMA as flame retardants.

As seen in **Figure 31**, there is a density gradient in every scenario, indicating that the foam block's density rises from top to bottom. Foam contracts in direct proportion to density once gases are released. As the foam develops, it finally stops growing, lets out gases, shrinks, and accumulates mass in the bottom of the foam. This effect is also

influenced by particle dispersion. Because of the increased density, the particles gather close to the bottom [82].

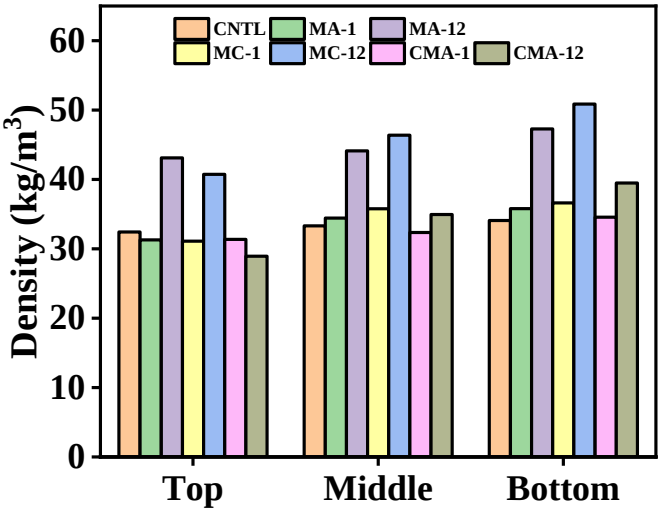

Figure 31: Apparent density of the obtained rigid PU foams with and without flame retardants (Top, Middle, and Bottom portions).

3.3.3. Closed Cell Content

Polymeric foams' capacity to withstand aging and maintain their thermal insulation qualities can be determined by counting the number of closed or open cells within the foam [83], [84]. A high closed-cell content in rigid polyurethane foams is one of the requirements for enhanced thermal insulation. Here, the air trapped in between the cells inhibits heat and oxygen from spreading quickly, restricts their transmission in empty gaps, and raises the thermal barrier [85]. The foam's density increase following MA addition resulted in a decrease in the CCC, surpassing 90 as shown in **Figure 32**. For MC-added foams, the CCC increased up to MC-7 (13.33 wt%

MC) concentration and then decreased at higher concentrations. The CCC of CMA-affected foams gradually decreased beyond CMA-7 (13.33wt % CMA). The consistently high CCC values on average indicated a restriction in airflow within the foam's cellular structure, a crucial factor in preventing oxygen diffusion when the RPUF is exposed to a flame [36].

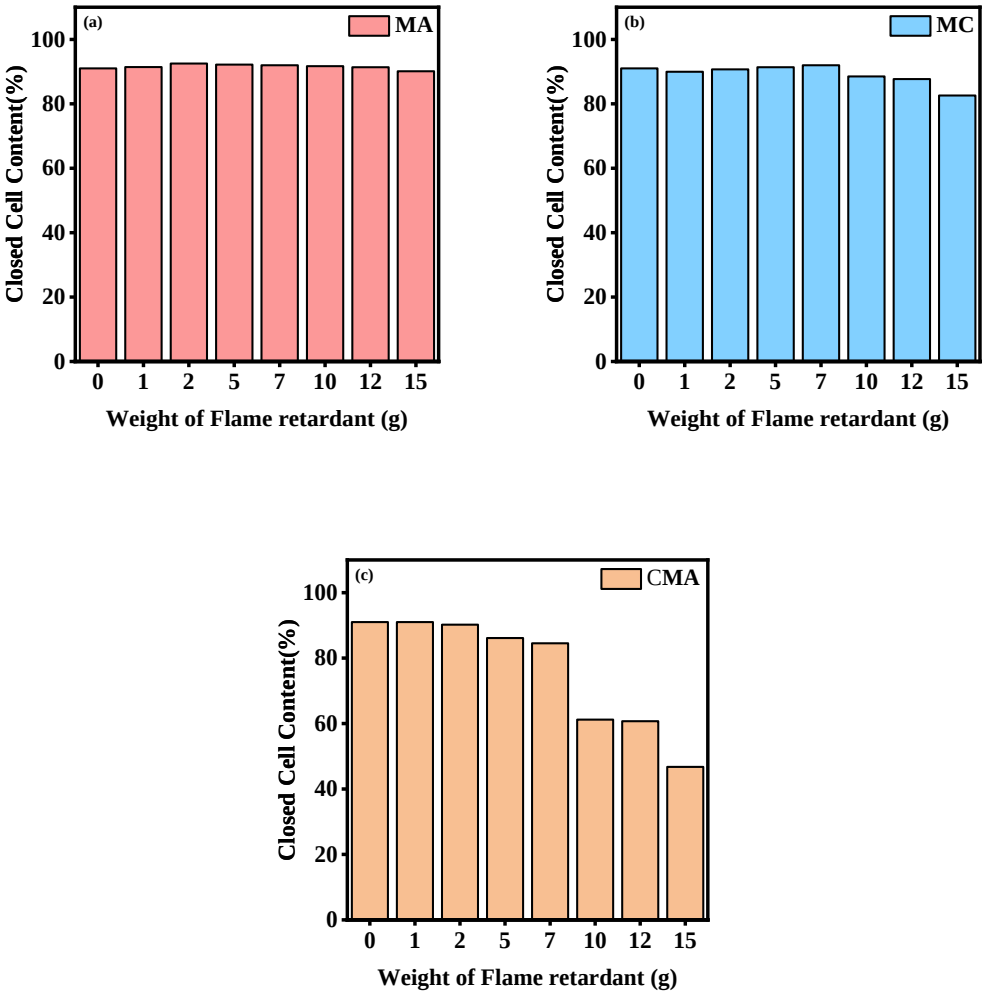

Figure 32: Closed-cell content of the obtained rigid PU foams with different weights of (a) MA, (b) MC, and (c) CMA as flame retardants.

As density increased from top to bottom, the closed cell content decreased which was shown in **Figure 33**.

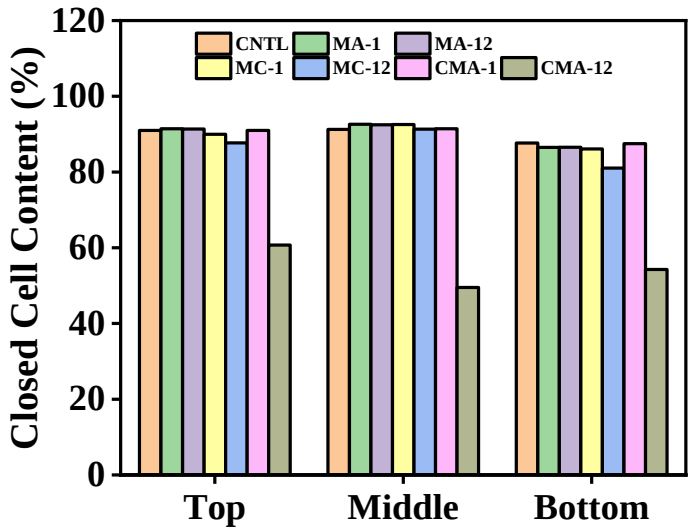

Figure 33: Closed cell content of the obtained rigid PU foams with and without flame retardants (Top, Middle, and Bottom portions).

3.3.4. Mechanical Properties of SBO-Based RPUF

3.3.4.1. Compression Strength

The rigid SBO foams' compression strength was evaluated at various flame-retardant concentrations. To investigate the impacts of the various flame retardants, the compressive strength at which the foams do not return to their former shapes was measured and compared in this analysis. This figure was seen, on average, following a 10% compression or strain. The compressive strength of rigid polyurethane foams is important for evaluating their mechanical characteristics. **Figure 34** shows that, although there are relatively few variations in the compressive strengths of the foams

containing FR, the general trend indicates that adding large loadings of FR reduces the foams' compressive strength.

Consequently, the variable compressive strength outcomes were evident in both MA and MC scenarios. However, a decrease in strength was observed at higher concentrations, specifically in MA-15 and MC-15 (28.56 wt% MA and MC), likely attributed to partial cell disruption. The foams' compressive strength exhibited a gradual decline with increasing CMA concentration. This reduction in compressive strength at higher CMA concentrations may be linked to the plasticizing effect of the P=O groups, which tends to decrease rigidity and introduce more flexibility into the polyurethane (PU) matrix during the curing process [36]. Inadequate interactions between CMA and RPUF, along with the presence of a flake-like structure, contribute to microphase separation, thereby diminishing the mechanical strength of the RPUF [80], [86]. Moreover, SEM analysis revealed that an increase in flame retardant concentration resulted in larger cell sizes and partial disruption of the cellular structure. This reduction in the number of cells in the foam led to an anticipated decrease in compressive strength [80].

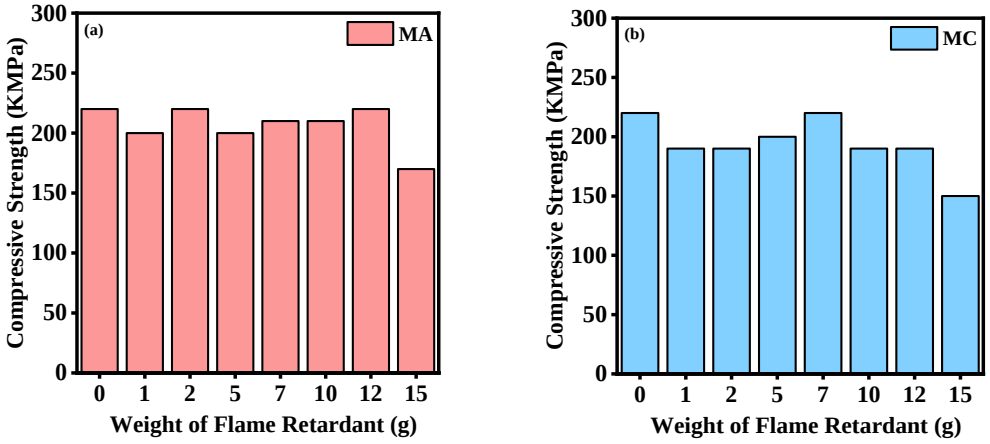

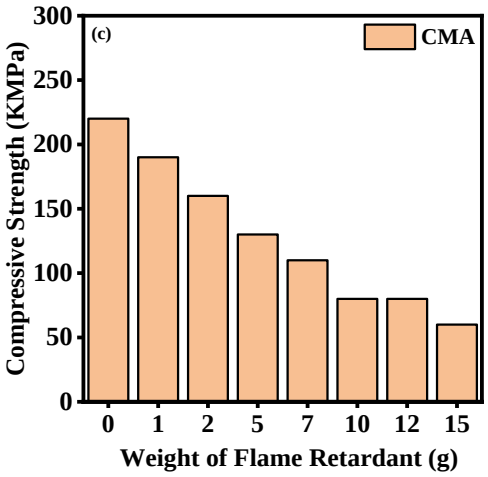

Figure 34: Compressive strength of rigid foams with different weights of (a) MA, (b) MC, and (c) CMA flame retardants.

Additionally in **Figure 35**, it has demonstrated a greater compression strength, particularly in the lower layers, which is consistent with a higher density. The decrease in cellular structure and propensity for solidification will directly correlate with an increase in compression strength [87]. The mold size may also matter since the walls of the mold could obstruct the flow of polymer during the foaming process. This restricted flow may cause gradients and differences in the mechanical and physical properties, which could affect the cells' size and shape [88]. The SEM pictures in **Figures 26, 27, 28,** and **29** which display subtle differences in the cellular architectures and foam appearances, further corroborate this.

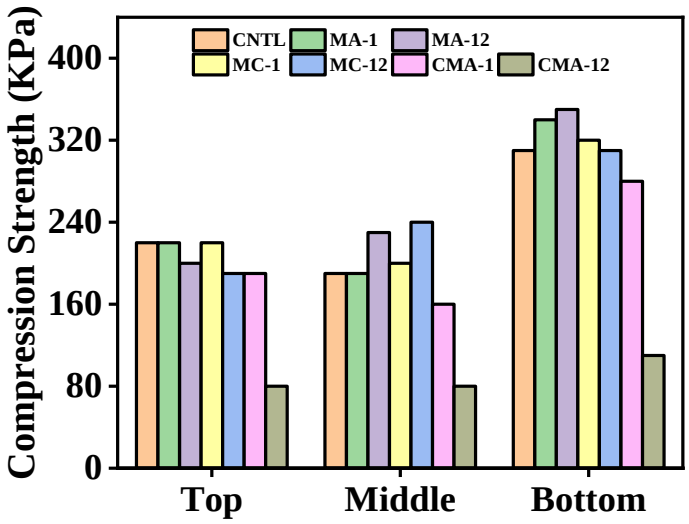

Figure 35: Compressive strength of obtained rigid foams with and without flame retardants (Top, Middle, and Bottom portions).

3.3.5. Flame-Retardant Behavior

3.3.5.1. Horizontal Burning Test

Since the primary purpose of a flame retardant is to prevent or delay flashover from flammable surfaces, its goal is not only to stop the polymer from igniting but also to slow down the rate of flame spread and prevent prolonged burning [89]. To determine the impact of MA, MC, and CMA on the thermal stability and flame-retardant qualities of rigid foams, the rigid foams manufactured using polyol from SBO were subjected to an open flame for 10 seconds during the horizontal burning test. **Figures 36, 37, 38,** and **39** illustrate the weight of the foam both before and after burning, along with the duration of time it took for the flame to go out.

After the ignition source was turned off, the foam without FR burned for 60.3 seconds. However, the burning times of the foams with FR were drastically shortened to 20.3 seconds for MA-5 (9.52 wt%), 36.05 seconds for MC-7 (13.33 wt%), and 31.85 seconds for MCA-5 (9.52 wt%) when MA, MC, and CMA were added separately. At 28.56 weight percentage FR, the lowest values of these times were found in MA-15 at 10.1 s, MC-15 at 28.4 s, and CMA-15 at 15.25 s. The trend in the burning time with an increase in MA, MC, and CMA can be used to explain the weight loss in **Figures 36b, 37b, 38b,** and **39b**. Here, the foam without FR lost 55.47% of its weight; this dropped to about 5% in MA, 13% in MC, and 8% in CMA. This suggests that the non-halogenated FR's presence had a major impact on the foam's capacity to burn down.

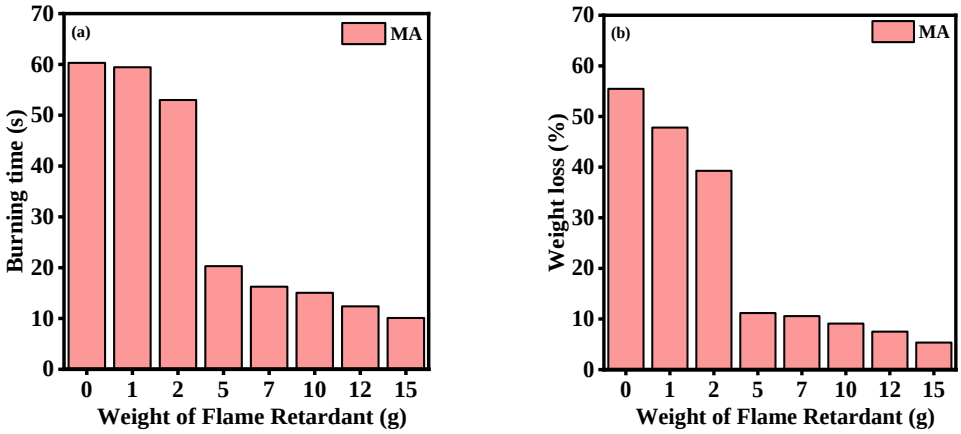

Figure 36: Comparisons of (a) burning time and (b) weight loss percent with different weights of MA.

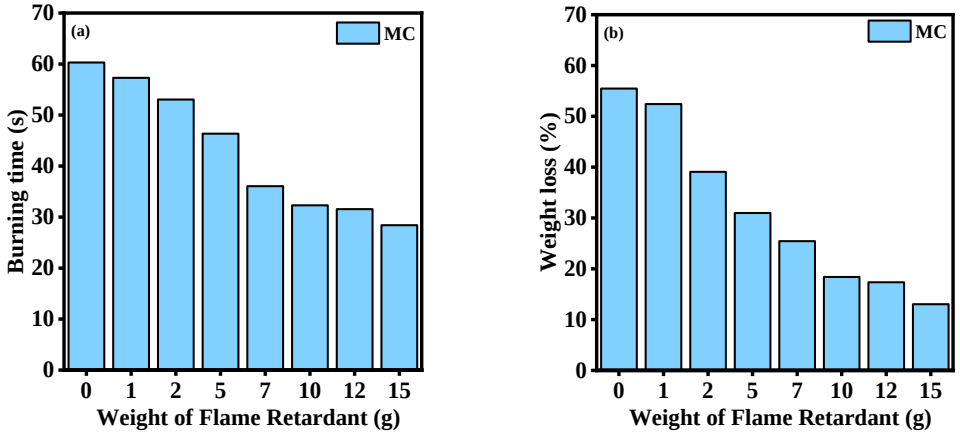

Figure 37: Comparisons of (a) burning time and (b) weight loss percent with different weights of MC.

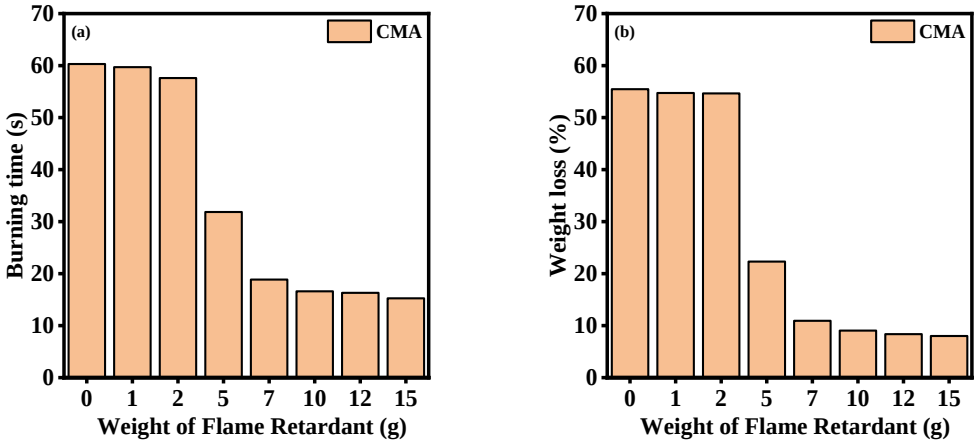

Figure 38: Comparisons of (a) burning time and (b) weight loss percent with different weights of CMA.

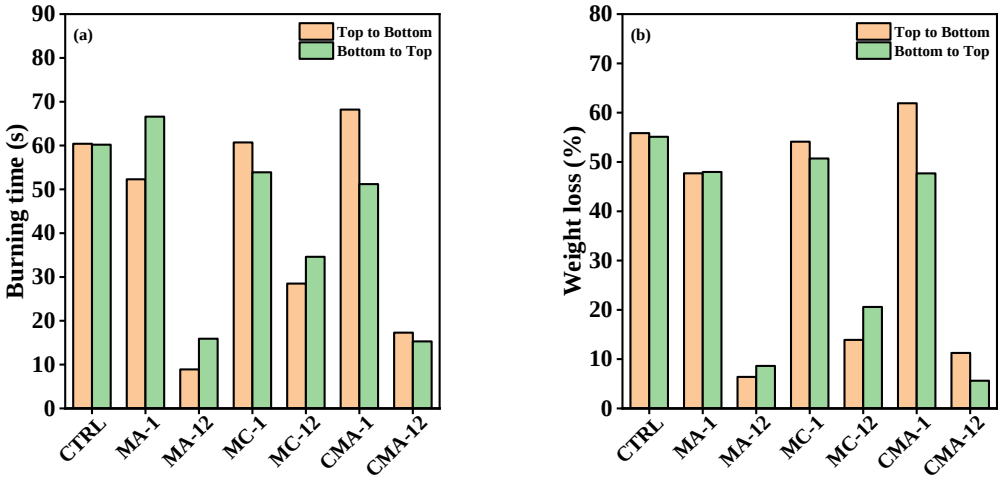

Figure 39: Comparisons of (a) burning time and (b) weight loss percent with and without FRs (Top to bottom and Bottom to Top).

Figures 40, 41, and **42** depict images from the horizontal burning of the foams, which clearly illustrate this behavior. It shows a full burning pattern of the foam without FR and a decrease in the burned fraction of the SBO foams with an increase in MA, MC, and CMA. Most FRs interfere with one or more of the three fundamental supports of combustion: heat, fuel, and oxygen; MA and its derivative (MC) interfere with all three. It first creates a heat sink by indulging in endothermic reactions and the subsequent breakdown of melamine vapors. It provides only approximately 40% of the heat needed for the burning of hydrocarbons; thus, nitrogen and ammonia, which act as inert diluents, are created [90]. Nitrogen-based flame retardants (MA, MC, and CMA) function by either causing inert gases, including nitrogen and ammonia, to be released into the gas phase or by condensation processes occurring in the solid phase.

MA can also play a major role in the formation of a char layer during the intumescent phase. The char layer serves as a partition between the gases generated

during the breakdown of polymers and oxygen. When paired with phosphorous synergists, MA can further enhance char stability through the formation of nitrogen-phosphorous compounds. To increase the char layer's ability to act as a heat barrier, MA and MC can also act as blowing agents for the char.

Due to its phosphorous-nitrogen base, CMA can burn into N_2 and NH_3 as well as pieces of the PO_2 and PO_3 radicals. As the polyurethane foams burn, they also release free radicals that are ignitable and flammable. However, some extremely exothermic free radical fragments, such OH• and H•, that are produced during the PU combustion are prevented from reigniting the PU matrix by the presence of PO_2• and other free radical fragments from CMA, which function as radical scavengers [84]. By keeping these reactive species away from the PU matrix, it can slow down the rate of burning and increase the foams' flame retardancy. The gas phase is the term for this type of FR process. Furthermore, phosphorous acid was also produced in the solid-phase mechanism of CMA, which can promote charring-a protective layer created during burning-to prevent further degradation of the remaining foams by shielding the underlying material from heat and acting as a barrier to the surface release of fuel gases [91]–[94].

Figure 40: Digital Photographs of SBO-RPUFs after the horizontal burning test with different concentrations of MA.

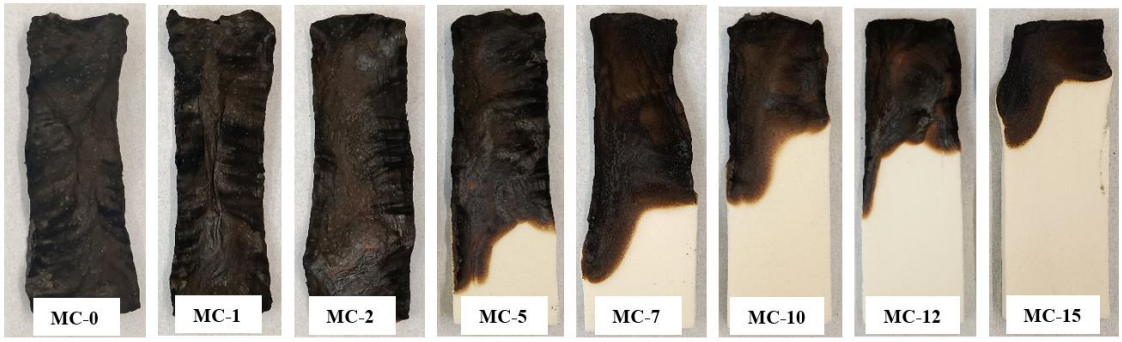

Figure 41: Digital Photographs of SBO-RPUFs after the horizontal burning test with different concentrations of MC.

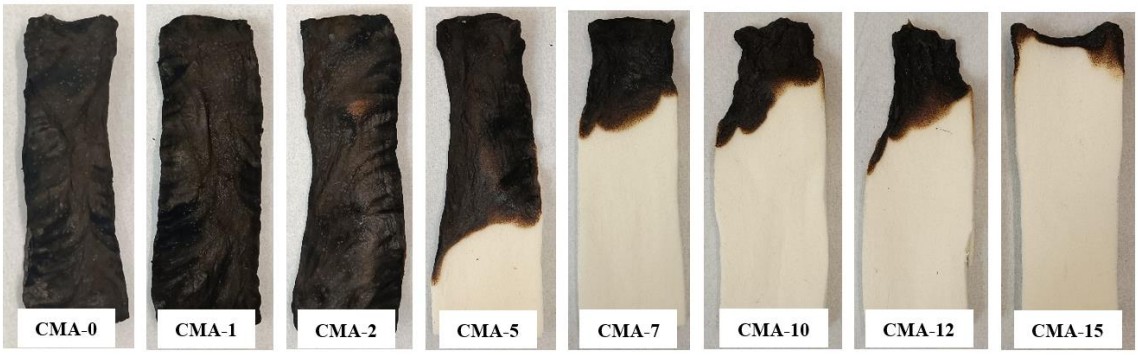

Figure 42: Digital Photographs of SBO-RPUFs after the horizontal burning test with different concentrations of CMA.

3.3.6. Thermal Stability

3.3.6.1. Thermogravimetric Analysis

Thermogravimetric analysis (TGA) was used to characterize the thermal degradation behavior of RPUFs. **Figures 43, 44, 45,** and **46** displayed the resulting TGA curves under nitrogen. There are two to three steps involved in the heat breakdown of polyurethanes [95]–[97]. The two-stage deterioration process that the RPUF went through in MA at different temperatures between 220 and 400 °C. Two primary stages of heat degradation could be distinguished in MC containing RPUF samples, at 220-380 and 380-520 °C. Lower temperatures cause the initial weight loss because any

volatile substances or moisture in the sample evaporate. The first maximum mass loss is caused by the breakdown of the polyurethane bond, which releases isocyanate, alcohol, primary and/or secondary amine, olefin, and carbon dioxide when hard segments fail [20], [40], [98]. The second maximal deterioration step was the heat-induced breakdown of the soft segments [94]. When MC in the foam breaks down, nitrogen-containing substances such as melamine and cyanuric acid are released. The release of NH_3, which may reduce the oxygen content surrounding the matrix, is the primary reason why nitrogen-based FRs (MA and MC) are important in the gas phase [99]. Furthermore, because of the formation of more thermally stable polymeric compounds like melam, melem, and melon, it has little effect on the condensed phase [74].

Flame-retardant RPUF broke down in four stages in CMA, at temperatures ranging from 100–150, 180–250, 250–360, and 360–500 °C, in that order. The initial loss of CMA's weight was ascribed to the flame-retardant RPUF breaking down between 100 and 150 °C. As the concentration of CMA in RPUF rose, the first degradation peak of RPUF gradually broadened. The breakdown of the RPUF foam with CMA caused the second deterioration stage, which happened between 180 and 250 °C; this peak extended as CMA loadings in RPUF rose. The third deterioration step was mostly caused by the depolymerization of polyurethane, which broke down the polyurethane linkage into isocyanate, polyol, primary or secondary amine, olefin, and carbon dioxide [100]. The final stage of deterioration was caused by the isocyanate dimerization and trimerization process as well as the heat breakdown of the soft segments [101]. The elimination of adsorbed water, the breakage of the P−C bond in

CMA, the breaking of the ionic bond between $-COO^-$ and RNH_3^+, the further formation of cross-linked 2-carboxyethyl-(phenyl)phosphinic acid (CEPP) and melamine derivatives, and finally the formation of polyphosphoric acid were the reasons for the maximum weight loss temperatures of CMA [58], [76]. Derivatives of phosphinic acid, a potent Lewis acid catalyst, were formed, which hastened the breakdown of RPUF. Further peaks, which may be the result of unreacted chemicals and FR degradation, were discovered at 240–260 °C in MA-containing foams at greater concentrations and 320–340 °C in RPUFs without FR and with MA, MC, and CMA. As the foam heats down, the other components may leave behind residues. There could be extra peaks in the TGA curve because of these residues breaking down at various temperatures.

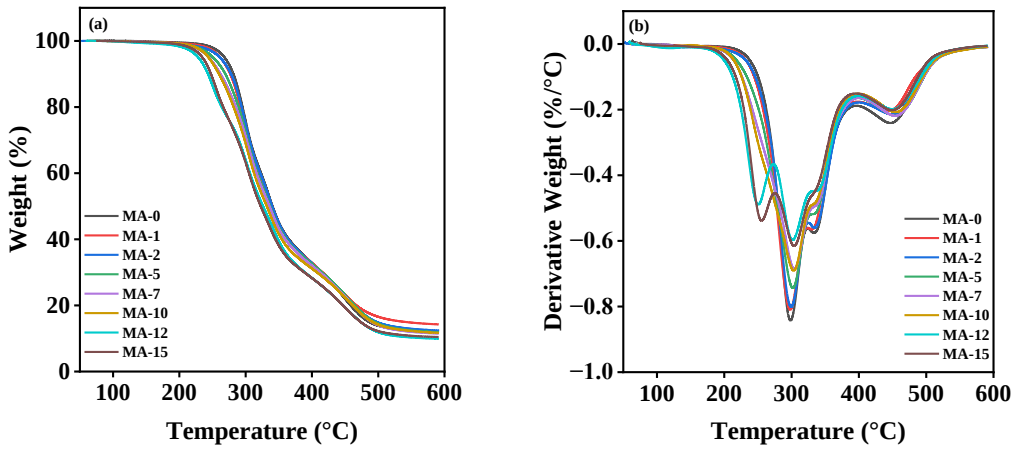

Figure 43. Thermal analysis of foams with varying amounts of MA (a) TGA, (b) DTGA.

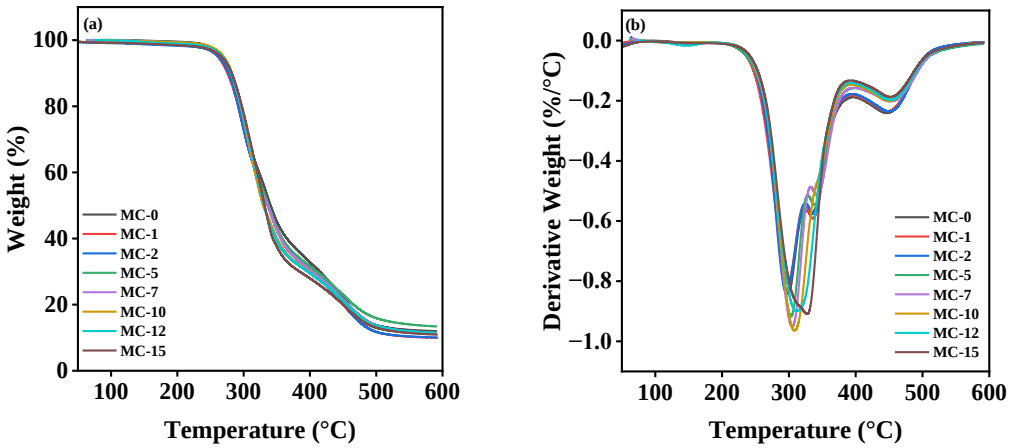

Figure 44. Thermal analysis of foams with varying amounts of MC (a) TGA, (b) DTGA.

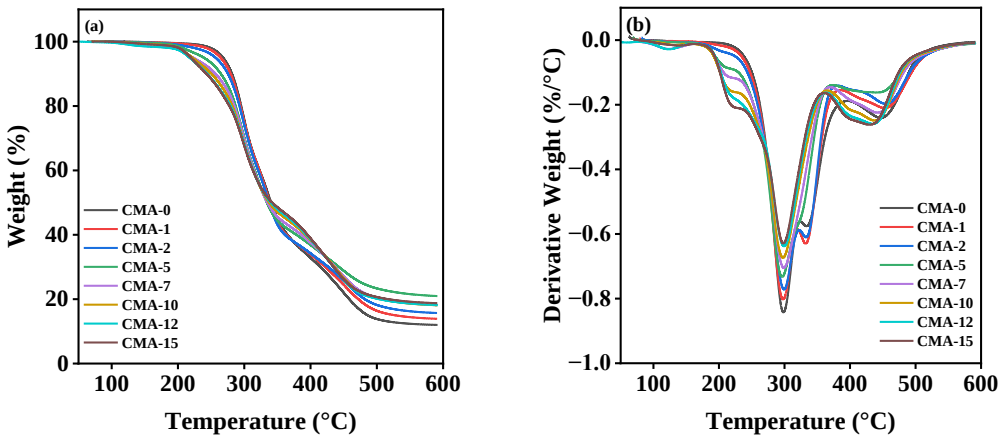

Figure 45. Thermal analysis of foams with varying amounts of CMA (a) TGA, (b) DTGA.

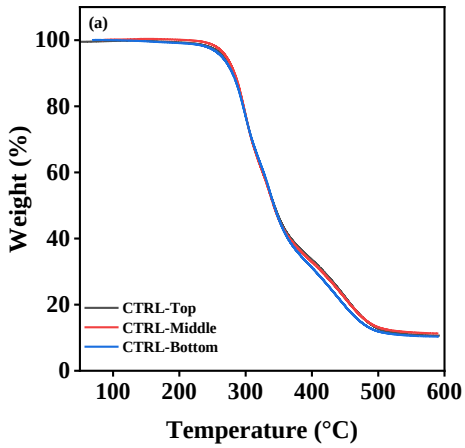
(a)
Weight (%)
Temperature (°C)
CTRL-Top
CTRL-Middle
CTRL-Bottom

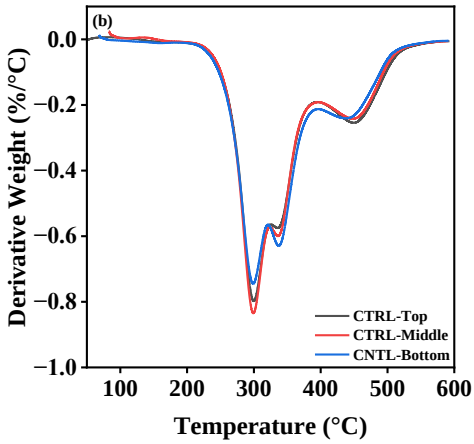
(b)
Derivative Weight (%/°C)
Temperature (°C)
CTRL-Top
CTRL-Middle
CNTL-Bottom

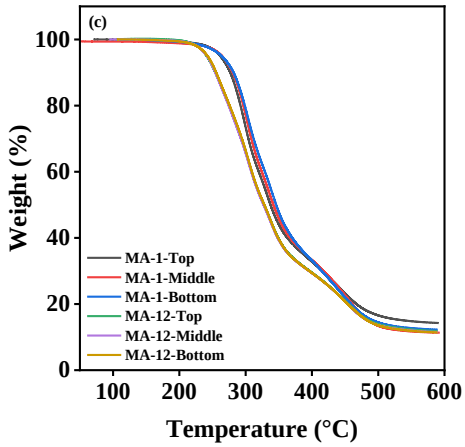
(c)
Weight (%)
Temperature (°C)
MA-1-Top
MA-1-Middle
MA-1-Bottom
MA-12-Top
MA-12-Middle
MA-12-Bottom

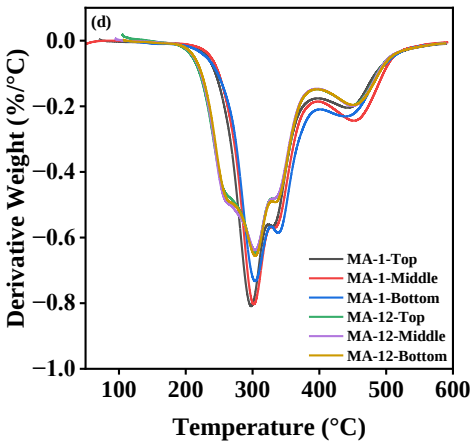
(d)
Derivative Weight (%/°C)
Temperature (°C)
MA-1-Top
MA-1-Middle
MA-1-Bottom
MA-12-Top
MA-12-Middle
MA-12-Bottom

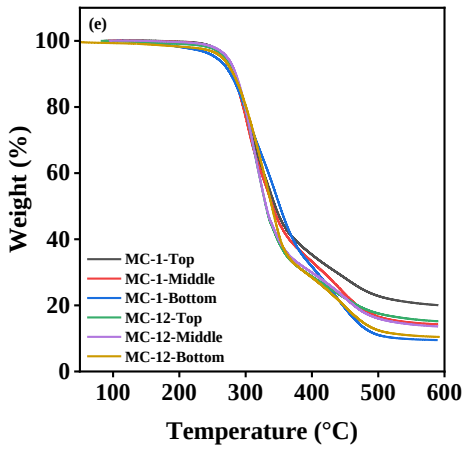
(e)
Weight (%)
Temperature (°C)
MC-1-Top
MC-1-Middle
MC-1-Bottom
MC-12-Top
MC-12-Middle
MC-12-Bottom

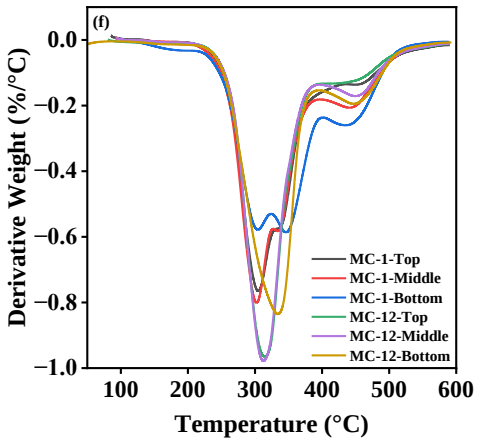
(f)
Derivative Weight (%/°C)
Temperature (°C)
MC-1-Top
MC-1-Middle
MC-1-Bottom
MC-12-Top
MC-12-Middle
MC-12-Bottom

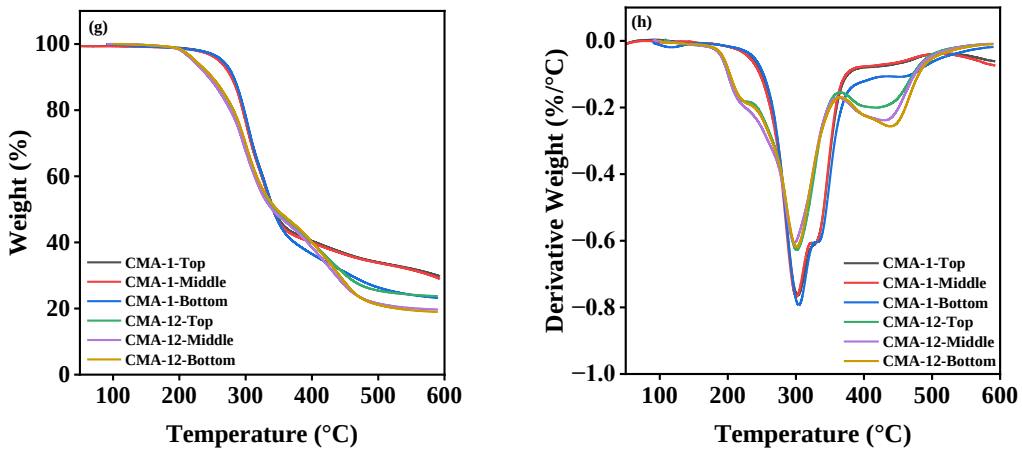

Figure 46. Thermal analysis of foams with and without FRs (Top, Middle, and Bottom) (a, c, e, and g) TGA, and (b, d, f, and h) DTGA.

Melamine was shown to have better thermal stability and fire resistance based on the studies above, which also looked at flame retardancy and physical attributes. The addition of FRs resulted in a significant improvement in the flame-retardant behavior of RPUFs. But when it came to its ability to put out fires, a comparatively modest concentration of MA-5 (9.5 wt %) produced the best results, followed by CMA. In contrast to MA and CMA, MC required higher concentrations to provide the same level of flame retardancy. The other 2 FRs, CMA and MC, promoted a much lesser drop in mechanical properties in comparison to MA. The synthesized RPUF in this work showed a significantly reduced density, which is important for construction-related applications. However, a comparison of MA, MC, and CMA revealed that MA had a far smaller detrimental effect on the RPUF's compression strength.

CHAPTER IV

CONCLUSIONS

The SBO-polyol was successfully synthesized, and in addition to the non-halogenated FRs, MA, MC, and CMA in increasing proportions, the synthesis of the SBO foam was ultimately successful. The density of the foams was in the range of 31-47 kg/m^3 in MA, 31-44 kg/m^3 in MA and that of CMA was between 28-31 kg/m^3, which falls within the acceptable range for a variety of rigid foam applications. The foams had CCCs greater than 90 in MA and less in MC and CMA when compared. In comparison to the control sample, MA-15 exhibited an 83% reduction in burning time, whereas MC-15 and CMA-15 showed respective decreases of 53% and 75%. As a result, the FRs showed an increase in flame retardancy and thermal stability of the SBO-RPUF therefore, it was evident that MA, MC, and CMA are more environmentally friendly choices than halogenated FRs. However, upon comparative analysis, it became evident that the MA derivatives (MC and CMA) exhibited diminished efficacy in enhancing the foam's fire-retardant capabilities of RPUFs in contrast to the unmodified MA. Additionally, significantly smaller quantities were needed to attain the best performance, which suggests a reduction in cost because subsequent addition produces results with little variance. Using that as a foundation, this work offers a practical and adjustable process for the creation of a more sustainable RPUF generated from SBO, along with the

addition of effective FR characteristics, which can broaden its range of uses in diverse scenarios.

Future Suggestions

a) Using this as a foundation, this work offers a practical and adjustable process for creating a more sustainable RPUF generated from SBO, and adding other flame retardants could broaden its range of uses in diverse scenarios.

b) Future studies should explore the environmental impact and sustainability aspects of using soybean oil-based polyols in rigid polyurethane foam production compared to conventional petrochemical-based counterparts.

c) Conducting comparative studies with other bio-based polyols and flame retardants to assess their performance and environmental impact can help identify the most suitable materials for specific applications.

d) Analyze the volatiles produced by the foams made from soybean oil that were burned horizontally and by TGA analysis.

e) Examine the scalability of foams made from soybean oil and research the entire life cycle of the product, including recycling.

REFERENCES

[1] B. Otto and B. Farbenfabriken, "A N G E W A N D T E C H E M I E Das Di-lsocganat-Poluadditionsverfahren (Polyurethane)," *Angew. Chemie*, vol. 59, no. 9, pp. 257–288, 1947.

[2] A. Das and P. Mahanwar, "A brief discussion on advances in polyurethane applications," *Adv. Ind. Eng. Polym. Res.*, vol. 3, no. 3, pp. 93–101, 2020, doi: 10.1016/j.aiepr.2020.07.002.

[3] C. Zhang and M. R. Kessler, "Bio-based polyurethane foam made from compatible blends of vegetable-oil-based polyol and petroleum-based polyol," *ACS Sustain. Chem. Eng.*, vol. 3, no. 4, pp. 743–749, 2015, doi: 10.1021/acssuschemeng.5b00049.

[4] U. Šebenik and M. Krajnc, "Influence of the soft segment length and content on the synthesis and properties of isocyanate-terminated urethane prepolymers," *Int. J. Adhes. Adhes.*, vol. 27, no. 7, pp. 527–535, 2007, doi: 10.1016/j.ijadhadh.2006.10.001.

[5] F. M. De Souza, P. K. Kahol, and R. K. Gupta, "Introduction to Polyurethane Chemistry," *ACS Symp. Ser.*, vol. 1380, pp. 1–24, 2021, doi: 10.1021/bk-2021-1380.ch001.

[6] J. O. Akindoyo, M. D. H. Beg, S. Ghazali, M. R. Islam, N. Jeyaratnam, and A. R. Yuvaraj, "Polyurethane types, synthesis and applications-a review," *RSC Adv.*, vol. 6, no. 115, pp. 114453–114482, 2016, doi: 10.1039/c6ra14525f.

[7] P. Cinelli, I. Anguillesi, and A. Lazzeri, "Green synthesis of flexible polyurethane foams from liquefied lignin," *Eur. Polym. J.*, vol. 49, no. 6, pp.

1174–1184, Jun. 2013, doi: 10.1016/J.EURPOLYMJ.2013.04.005.

[8] N. V. Gama *et al.*, “Bio-based polyurethane foams toward applications beyond thermal insulation,” *Mater. Des.*, vol. 76, pp. 77–85, 2015, doi: 10.1016/j.matdes.2015.03.032.

[9] A. Bîrca, O. Gherasim, V. Grumezescu, and A. M. Grumezescu, “Introduction in thermoplastic and thermosetting polymers,” *Mater. Biomed. Eng. Thermoset Thermoplast. Polym.*, pp. 1–28, 2019, doi: 10.1016/B978-0-12-816874-5.00001-3.

[10] M. F. Sonnenschein, *Polyurethanes: Science, Technology, Markets, and Trends*, 1st ed. MI, USA: John Wiley & Sons, Inc., 2015.

[11] H. Benes, J. Rosner, P. Holer, H. Synkova, J. Kotek, and Z. Horak, “Glycolysis of flexible polyurethane foam in recycling of car seats,” *Polym. Adv. Technol.*, 2006, doi: 10.1002/pat.

[12] Y. Deng, R. Dewil, L. Appels, R. Ansart, J. Baeyens, and Q. Kang, “Reviewing the thermo-chemical recycling of waste polyurethane foam,” *J. Environ. Manage.*, vol. 278, no. P1, p. 111527, 2021, doi: 10.1016/j.jenvman.2020.111527.

[13] N. V. Gama *et al.*, “Thermal energy storage and mechanical performance of crude glycerol polyurethane composite foams containing phase change materials and expandable graphite,” *Materials (Basel).*, vol. 11, no. 10, 2018, doi: 10.3390/ma11101896.

[14] T. A. P. Hai *et al.*, “Renewable polyurethanes from sustainable biological precursors,” *Biomacromolecules*, vol. 22, no. 5, pp. 1770–1794, 2021, doi:

10.1021/acs.biomac.0c01610.

[15] A. Gomez-Lopez, B. Grignard, I. Calvo, C. Detrembleur, and H. Sardon, “Monocomponent Non-isocyanate Polyurethane Adhesives Based on a Sol-Gel Process,” *ACS Appl. Polym. Mater.*, vol. 2, no. 5, pp. 1839–1847, 2020, doi: 10.1021/acsapm.0c00062.

[16] R. Kaur, P. Singh, S. Tanwar, G. Varshney, and S. Yadav, “Assessment of Bio-Based Polyurethanes: Perspective on Applications and Bio-Degradation,” *Macromol*, vol. 2, no. 3, pp. 284–314, 2022, doi: 10.3390/macromol2030019.

[17] S. Wu, D. Deng, L. Zhou, P. Zhang, and G. Tang, “Flame retardancy and thermal degradation of rigid polyurethane foams composites based on aluminum hypophosphite,” *Mater. Res. Express*, vol. 6, no. 10, 2019, doi: 10.1088/2053-1591/ab41b2.

[18] S. T. McKenna and T. R. Hull, “The fire toxicity of polyurethane foams,” *Fire Sci. Rev.*, vol. 5, no. 1, 2016, doi: 10.1186/s40038-016-0012-3.

[19] H. Singh and A. K. Jain, “Ignition, Combustion, Toxicity, and Fire Retardancy of Polyurethane Foams: A Comprehensive Review,” *Wiley Intersci.*, 2008, doi: 10.1002/app.

[20] X. Liu, J. Hao, and S. Gaan, “Recent studies on the decomposition and strategies of smoke and toxicity suppression for polyurethane based materials,” *RSC Adv.*, vol. 6, no. 78, pp. 74742–74756, 2016, doi: 10.1039/c6ra14345h.

[21] Y. Hu, Y. Tian, J. Cheng, and J. Zhang, “Synthesis of Eugenol-Based Polyols via Thiol-Ene Click Reaction and High-Performance Thermosetting Polyurethane Therefrom,” *ACS Sustain. Chem. Eng.*, vol. 8, no. 10, pp. 4158–

4166, 2020, doi: 10.1021/acssuschemeng.9b06867.

[22] B. V Tawade *et al.*, "Bio-Based Di-/Poly-isocyanates for Polyurethanes: An Overview," *PU Today*, no. 4, pp. 41–46, 2017, doi: 10.13140/RG.2.2.20183.98726/2.

[23] S. Schmidt, B. S. Ritter, D. Kratzert, B. Bruchmann, and R. Mülhaupt, "Isocyanate-free route to poly(carbohydrate-urethane) thermosets and 100% bio-based coatings derived from glycerol feedstock," *Macromolecules*, vol. 49, no. 19, pp. 7268–7276, 2016, doi: 10.1021/acs.macromol.6b01485.

[24] M. Ionescu, *Chemistry and Technology of Polyols for Polyurethanes , 2nd Edition*, vol. 2. 2016.

[25] D. P. Pfister, Y. Xia, and R. C. Larock, "Recent advances in vegetable oil-based polyurethanes," *ChemSusChem*, vol. 4, no. 6, pp. 703–717, 2011, doi: 10.1002/cssc.201000378.

[26] S. D. Bote and R. Narayan, "Synthesis of Biobased Polyols from Soybean Meal for Application in Rigid Polyurethane Foams," *Ind. Eng. Chem. Res.*, vol. 60, no. 16, pp. 5733–5743, 2021, doi: 10.1021/acs.iecr.0c06306.

[27] R. K. Gupta, Ed., *Specialty Polymers: Fundamentals, Properties, Applications and Advances*. Boca Raton, FL: CRC Press, 2023. doi: https://doi.org/10.1201/9781003278269.

[28] M. A. Asare, F. M. de Souza, and R. K. Gupta, "Waste to Resource: Synthesis of Polyurethanes from Waste Cooking Oil," *Ind. Eng. Chem. Res.*, vol. 61, p. 18400, 2022.

[29] V. Suthar, M. A. Asare, P. Sahu, and R. K. Gupta, "Sunflower oil-based

polyurethane/graphene composite: Synthesis and properties," *J. Thermoplast. Compos. Mater.*, p. 08927057231202408, Sep. 2023, doi: 10.1177/08927057231202408.

[30] M. A. Asare, P. Kote, S. Chaudhary, F. M. de Souza, and R. K. Gupta, "Sunflower Oil as a Renewable Resource for Polyurethane Foams: Effects of Flame-Retardants," *Polymers (Basel).*, vol. 14, no. 23, p. 5282, 2022.

[31] A. D. Macalino, V. A. Salen, and L. Q. Reyes, "Castor Oil Based Polyurethanes: Synthesis and Characterization," *IOP Conf. Ser. Mater. Sci. Eng.*, vol. 229, no. 1, 2017, doi: 10.1088/1757-899X/229/1/012016.

[32] S. Bhoyate, M. Ionescu, P. K. Kahol, and R. K. Gupta, "Castor-oil derived nonhalogenated reactive flame-retardant-based polyurethane foams with significant reduced heat release rate," *J. Appl. Polym. Sci.*, vol. 136, no. 13, p. 47276, 2019.

[33] A. Guo, Y. Cho, and Z. S. Petrović, "Structure and properties of halogenated and nonhalogenated soy-based polyols," *J. Polym. Sci. Part A Polym. Chem.*, vol. 38, no. 21, pp. 3900–3910, 2000, doi: 10.1002/1099-0518(20001101)38:21<3900::AID-POLA70>3.0.CO;2-E.

[34] Z. Fang *et al.*, "Development of High-Performance Biodegradable Rigid Polyurethane Foams Using Full Modified Soy-Based Polyols," *J. Agric. Food Chem.*, vol. 67, no. 8, pp. 2220–2226, 2019, doi: 10.1021/acs.jafc.8b05342.

[35] M. B. Figueirêdo, I. Hita, P. J. Deuss, R. H. Venderbosch, and H. J. Heeres, "Pyrolytic lignin: a promising biorefinery feedstock for the production of fuels and valuable chemicals," *Green Chem.*, vol. 24, no. 12, pp. 4680–4702, Jan.

2022, doi: 10.1039/D2GC00302C.

[36] C. Zhang, S. Bhoyate, M. Ionescu, P. K. Kahol, and R. K. Gupta, “Highly flame retardant and bio-based rigid polyurethane foams derived from orange peel oil,” *Polym. Eng. Sci.*, vol. 58, no. 11, pp. 2078–2087, 2018, doi: 10.1002/pen.24819.

[37] M. A. Sawpan, “Polyurethanes from vegetable oils and applications: a review,” *J. Polym. Res.*, vol. 25, no. 8, 2018, doi: 10.1007/s10965-018-1578-3.

[38] J. Peyrton and L. Avérous, “Structure-properties relationships of cellular materials from biobased polyurethane foams,” *Mater. Sci. Eng. R Reports*, vol. 145, no. February, 2021, doi: 10.1016/j.mser.2021.100608.

[39] M. L. Pinto, “Formulation, preparation, and characterization of polyurethane foams,” *J. Chem. Educ.*, vol. 87, no. 2, pp. 212–215, 2010, doi: 10.1021/ed8000599.

[40] D. K. Chattopadhyay and D. C. Webster, “Thermal stability and flame retardancy of polyurethanes,” *Prog. Polym. Sci.*, vol. 34, no. 10, pp. 1068–1133, 2009, doi: 10.1016/j.progpolymsci.2009.06.002.

[41] H. R. L., *Szycher’s Handbook of Polyurethanes*. 1999. doi: 10.1038/142853a0.

[42] E. Sharmin and F. Zafar, “Chapter 1 :Polyurethane: An Introduction,” *Polyurethane*, pp. 1–14, 2012, [Online]. Available: https://cdn.intechopen.com/pdfs/38589/InTech-Polyurethane_an_introduction.pdf

[43] N. V. Gama, A. Ferreira, and A. Barros-Timmons, “Polyurethane foams: Past, present, and future,” *Materials (Basel).*, vol. 11, no. 10, 2018, doi: 10.3390/ma11101841.

[44] C. Carré, L. Bonnet, and L. Avérous, “Original biobased nonisocyanate polyurethanes: Solvent- and catalyst-free synthesis, thermal properties and rheological behaviour,” *RSC Adv.*, vol. 4, no. 96, pp. 54018–54025, 2014, doi: 10.1039/c4ra09794g.

[45] M. Janvier, P. H. Ducrot, and F. Allais, “Isocyanate-Free Synthesis and Characterization of Renewable Poly(hydroxy)urethanes from Syringaresinol,” *ACS Sustain. Chem. Eng.*, vol. 5, no. 10, pp. 8648–8656, 2017, doi: 10.1021/acssuschemeng.7b01271.

[46] Z. Wang, X. Zhang, L. Zhang, T. Tan, and H. Fong, “Nonisocyanate Biobased Poly(ester urethanes) with Tunable Properties Synthesized via an Environment-Friendly Route,” *ACS Sustain. Chem. Eng.*, vol. 4, no. 5, pp. 2762–2770, 2016, doi: 10.1021/acssuschemeng.6b00275.

[47] F. Laoutid, L. Bonnaud, M. Alexandre, J. M. Lopez-Cuesta, and P. Dubois, “New prospects in flame retardant polymer materials: From fundamentals to nanocomposites,” *Mater. Sci. Eng. R Reports*, vol. 63, no. 3, pp. 100–125, 2009, doi: 10.1016/j.mser.2008.09.002.

[48] S. Bhoyate *et al.*, “Highly flame-retardant bio-based polyurethanes using novel reactive polyols,” *J. Appl. Polym. Sci.*, vol. 135, no. 12, 2018, doi: 10.1002/app.46027.

[49] D. B. Soni and G. Bhatt, “A Review on Flame Retardants Used in Polyurethane Foam,” *ECS Trans.*, vol. 107, no. 1, pp. 1153–1164, 2022, doi: 10.1149/10701.1153ecst.

[50] J. W. Mitchell, “The History and Future Trends of Non-Halogenated Flame

Retarded Polymers," *Non-Halogenated Flame Retard. Handb.*, pp. 1–16, 2014, doi: 10.1002/9781118939239.ch1.

[51] J. John, M. Bhattacharya, and R. B. Turner, "Characterization of polyurethane foams from soybean oil," *J. Appl. Polym. Sci.*, vol. 86, no. 12, pp. 3097–3107, 2002, doi: 10.1002/app.11322.

[52] P. Furtwengler and L. Avérous, "Renewable polyols for advanced polyurethane foams from diverse biomass resources," *Polym. Chem.*, vol. 9, no. 32, pp. 4258–4287, 2018, doi: 10.1039/c8py00827b.

[53] H. Zhu and S. Xu, "Preparation of Flame-Retardant Rigid Polyurethane Foams by Combining Modified Melamine-Formaldehyde Resin and Phosphorus Flame Retardants," *ACS Omega*, vol. 5, no. 17, pp. 9658–9667, 2020, doi: 10.1021/acsomega.9b03659.

[54] A. König, U. Fehrenbacher, T. Hirth, and E. Kroke, "Flexible polyurethane foam with the flame-retardant melamine," *J. Cell. Plast.*, vol. 44, no. 6, pp. 469–480, 2008, doi: 10.1177/0021955X08095502.

[55] V. Sangeetha, N. Kanagathara, R. Sumathi, N. Sivakumar, and G. Anbalagan, "Spectral and Thermal Degradation of Melamine Cyanurate," *J. Mater.*, vol. 2013, pp. 1–7, 2013, doi: 10.1155/2013/262094.

[56] M. Modesti and A. Lorenzetti, "Flame retardancy of polyisocyanurate-polyurethane foams: Use of different charring agents," *Polym. Degrad. Stab.*, vol. 78, no. 2, pp. 341–347, 2002, doi: 10.1016/S0141-3910(02)00184-2.

[57] W. Tao and J. Li, "Melamine cyanurate tailored by base and its multi effects on flame retardancy of polyamide 6," *Appl. Surf. Sci.*, vol. 456, no. June, pp. 751–

762, 2018, doi: 10.1016/j.apsusc.2018.06.215.

[58] M. Chen, Z. Shao, X. Wang, L. Chen, and Y. Wang, “Halogen-Free Flame-Retardant Flexible Polyurethane Foam with a Novel Nitrogen−Phosphorus Flame Retardant,” 2012.

[59] M. T. Benaniba, N. Belhaneche-Bensemra, and G. Gelbard, “Epoxidation of sunflower oil with peroxoacetic acid in presence of ion exchange resin by various processes,” *Energy Educ. Sci. Technol.*, no. 2, pp. 71–82, 2008.

[60] Z. Petrovic, A. Guo, and I. Javni, “Process for the preparation of vegetable oil-based polyols and electroninsulating casting compounds created from vegetable oil-based polyols,” no. 19, 2000.

[61] M. J. Lerma-García, G. Ramis-Ramos, J. M. Herrero-Martínez, and E. F. Simó-Alfonso, “Authentication of extra virgin olive oils by Fourier-transform infrared spectroscopy,” *Food Chem.*, vol. 118, no. 1, pp. 78–83, 2010, doi: 10.1016/j.foodchem.2009.04.092.

[62] P. Liang *et al.*, “The Use of Fourier Transform Infrared Spectroscopy for Quantification of Adulteration in Virgin Walnut Oil,” *J. Spectrosc.*, vol. 1, 2013, [Online]. Available: http://dx.doi.org/10.1016/j.foodcont.2008.09.022

[63] M. D. Guillén and N. Cabo, “Characterization of edible oils and lard by fourier transform infrared spectroscopy. Relationships between composition and frequency of concrete bands in the fingerprint region,” *JAOCS, J. Am. Oil Chem. Soc.*, vol. 74, no. 10, pp. 1281–1286, 1997, doi: 10.1007/s11746-997-0058-4.

[64] R. Md Salim, J. Asik, and M. S. Sarjadi, “Chemical functional groups of extractives, cellulose and lignin extracted from native Leucaena leucocephala

bark," *Wood Sci. Technol.*, vol. 55, no. 2, pp. 295–313, 2021, doi: 10.1007/s00226-020-01258-2.

[65] J. D'Souza, B. George, R. Camargo, and N. Yan, "Synthesis and characterization of bio-polyols through the oxypropylation of bark and alkaline extracts of bark," *Ind. Crops Prod.*, vol. 76, pp. 1–11, 2015, doi: 10.1016/j.indcrop.2015.06.037.

[66] H. Pawlik and A. Prociak, "Influence of Palm Oil-Based Polyol on the Properties of Flexible Polyurethane Foams," *J. Polym. Environ.*, vol. 20, no. 2, pp. 438–445, 2012, doi: 10.1007/s10924-011-0393-2.

[67] Q. Jiang, P. Xu, J. Feng, and M. Sun, "Application of Covalent Organic Porous Polymers-Functionalized Basalt Fibers for in-Tube Solid-Phase Microextraction," *Molecules*, vol. 25, no. 24, 2020, doi: 10.3390/MOLECULES25245788.

[68] T. Sheng-Long, M. Lian-Xin, S. Xiao-Guang, and T. Xu-Dong, "Thermolysis parameter and kinetic research in copolyamide 66 containing 2-carboxyethyl phenyl phosphinic acid," *High Perform. Polym.*, vol. 27, no. 1, pp. 65–73, 2015, doi: 10.1177/0954008314539358.

[69] Z. Yao, X. Liu, L. Qian, Y. Chen, B. Xu, and Y. Qiu, "Synthesis and characterization of aluminum 2-carboxyethyl-phenyl-phosphinate and its flame-retardant application in polyester," *Polymers (Basel).*, vol. 11, no. 12, pp. 1–14, 2019, doi: 10.3390/polym11121969.

[70] Y. Chen and Q. Wang, "Preparation, properties and characterizations of halogen-free nitrogen-phosphorous flame-retarded glass fiber reinforced polyamide 6 composite," *Polym. Degrad. Stab.*, vol. 91, no. 9, pp. 2003–2013, 2006, doi:

10.1016/j.polymdegradstab.2006.02.006.

[71] C. Ma, T.-R. Wu, and Y.-H. Peng, “Method for preparing melamine salt of bis-(pentaerythritol phosphate) phosphoric acid,” vol. 1, no. 12, pp. 1–4, 2004.

[72] Y. Liu and Q. Wang, “Catalytic action of phospho-tungstic acid in the synthesis of melamine salts of pentaerythritol phosphate and their synergistic effects in flame retarded polypropylene,” *Polym. Degrad. Stab.*, vol. 91, no. 10, pp. 2513–2519, Oct. 2006, doi: 10.1016/J.POLYMDEGRADSTAB.2006.03.009.

[73] A. König, U. Fehrenbacher, E. Kroke, and T. Hirth, “Thermal decomposition behavior of the flame retardant melamine in slabstock flexible polyurethane foams,” *J. Fire Sci.*, vol. 27, no. 3, pp. 187–211, 2009, doi: 10.1177/0734904108099329.

[74] B. V. Lotsch and W. Schnick, “New light on an old story: Formation of melam during thermal condensation of melamine,” *Chem. - A Eur. J.*, vol. 13, no. 17, pp. 4956–4968, 2007, doi: 10.1002/chem.200601291.

[75] L. Costa and G. Camino, “Thermal behavıour of melamıne,” *J. Therm. Anal.*, vol. 34, pp. 423–429, 1988.

[76] M. J. Chen *et al.*, “Influence of valence and structure of phosphorus-containing melamine salts on the decomposition and fire behaviors of flexible polyurethane foams,” *Ind. Eng. Chem. Res.*, vol. 53, no. 21, pp. 8773–8783, 2014, doi: 10.1021/ie500691p.

[77] W. Xing, H. Yuan, P. Zhang, H. Yang, L. Song, and Y. Hu, “Functionalized lignin for halogen-free flame retardant rigid polyurethane foam: Preparation, thermal stability, fire performance and mechanical properties,” *J. Polym. Res.*,

vol. 20, no. 9, pp. 1–12, 2013, doi: 10.1007/s10965-013-0234-1.

[78] J. J. Shea, “Polymeric foams: mechanisms and materials [Book review],” *IEEE Electr. Insul. Mag.*, vol. 21, no. 2, pp. 56–56, 2005, doi: 10.1109/mei.2005.1412232.

[79] T. Widya and C. W. Macosko, “Nanoclay-modified rigid polyurethane foam,” *J. Macromol. Sci. - Phys.*, vol. 44 B, no. 6, pp. 897–908, 2005, doi: 10.1080/00222340500364809.

[80] L. Zhang, M. Zhang, Y. Zhou, and L. Hu, “The study of mechanical behavior and flame retardancy of castor oil phosphate-based rigid polyurethane foam composites containing expanded graphite and triethyl phosphate,” *Polym. Degrad. Stab.*, vol. 98, no. 12, pp. 2784–2794, 2013, doi: 10.1016/j.polymdegradstab.2013.10.015.

[81] G. Camino, S. Duquesne, R. Delobel, B. Eling, C. Lindsay, and T. Roels, “Mechanism of Expandable Graphite Fire Retardant Action in Polyurethanes,” *ACS Symp. Ser.*, vol. 797, pp. 90–109, 2001, doi: 10.1021/bk-2001-0797.ch008.

[82] D. de Mello, S. H. Pezzin, and S. C. Amico, “The effect of post-consumer PET particles on the performance of flexible polyurethane foams,” *Polym. Test.*, vol. 28, no. 7, pp. 702–708, 2009, doi: 10.1016/j.polymertesting.2009.05.014.

[83] V. M. Gravit, O. Ogidan, and E. Znamenskaya, “Methods for determining the number of closed cells in rigid sprayed polyurethane foam,” *MATEC Web Conf.*, vol. 193, pp. 1–8, 2018, doi: 10.1051/matecconf/201819303027.

[84] F. Feng and L. Qian, “The Flame Retardant Behaviors and Synergistic Effect of Expandable Graphite and Dimethyl Methylphosphonate in Rigid Polyurethane

Foams," *Polym. Polym. Compos.*, vol. 35, p. 301−309, 2014, doi: 10.1002/pc.

[85] S. Tan, T. Abraham, D. Ference, and C. W. MacOsko, "Rigid polyurethane foams from a soybean oil-based Polyol," *Polymer (Guildf).*, vol. 52, no. 13, pp. 2840–2846, 2011, doi: 10.1016/j.polymer.2011.04.040.

[86] F. M. de Souza, J. Choi, S. Bhoyate, P. K. Kahol, and R. K. Gupta, "Mechanisms for flame retardancy," *C — J. Carbon Res.*, vol. 6, no. 2, p. 27, 2020, doi: 10.3390/c6020027.

[87] K. S. Chian and L. H. Gan, "Development of a rigid polyurethane foam from palm oil," *J. Appl. Polym. Sci.*, vol. 68, no. 3, pp. 509–515, 1998, doi: 10.1002/(SICI)1097-4628(19980418)68:3<509::AID-APP17>3.0.CO;2-P.

[88] D. Jackovich, B. O'Toole, M. C. Hawkins, and L. Sapochak, "Temperature and mold size effects on physical and mechanical properties of a polyurethane foam," *J. Cell. Plast.*, vol. 41, no. 2, pp. 153–168, 2005, doi: 10.1177/0021955X05051739.

[89] J. Green, "Mechanisms for flame retardancy and smoke suppression - A review," *J. Fire Sci.*, vol. 14, no. 6, pp. 426–442, 1996, doi: 10.1177/073490419601400602.

[90] J. Murphy, "Modifying Specific Properties: Flammability – Flame Retardants, Chapter in Additives for Plastics Handbook (Second Edition)", doi: 10.1016/B978-1-85617-370-4.50012-9.

[91] B. Dittrich, K. A. Wartig, R. Mülhaupt, and B. Schartel, "Flame-retardancy properties of intumescent ammonium poly(phosphate) and mineral filler magnesium hydroxide in combination with graphene," *Polymers (Basel).*, vol. 6,

no. 11, pp. 2875–2895, 2014, doi: 10.3390/polym6112875.

[92] B. Scharte, “Phosphorus-based flame retardancy mechanisms-old hat or a starting point for future development?,” *Materials (Basel).*, vol. 3, no. 10, pp. 4710–4745, 2010, doi: 10.3390/ma3104710.

[93] S. Duquesne *et al.*, “Mechanism of fire retardancy of polyurethanes using ammonium polyphosphate,” *J. Appl. Polym. Sci.*, vol. 82, no. 13, pp. 3262–3274, 2001, doi: 10.1002/app.2185.

[94] Y. W. Yan, L. Chen, R. K. Jian, S. Kong, and Y. Z. Wang, “Intumescence: An effect way to flame retardance and smoke suppression for polystryene,” *Polym. Degrad. Stab.*, vol. 97, no. 8, pp. 1423–1431, 2012, doi: 10.1016/j.polymdegradstab.2012.05.013.

[95] Z. S. Petrović, Z. Zavargo, J. H. Flyn, and W. J. Macknight, “Thermal degradation of segmented polyurethanes,” *J. Appl. Polym. Sci.*, vol. 51, no. 6, pp. 1087–1095, 1994, doi: 10.1002/app.1994.070510615.

[96] N. Grassie and G. A. Perdomo Mendoza, “Thermal degradation of polyether-urethanes: 5. Polyether-urethanes prepared from methylene bis(4-phenylisocyanate) and high molecular weight poly(ethylene glycols) and the effect of ammonium polyphosphate,” *Polym. Degrad. Stab.*, vol. 11, no. 4, pp. 359–379, Jan. 1985, doi: 10.1016/0141-3910(85)90039-4.

[97] Y. Zhang, S. Shang, X. Zhang, D. Wang, and D. J. Hourston, “Influence of structure of hydroxyl-terminated maleopimaric acid ester on thermal stability of rigid polyurethane foams,” *J. Appl. Polym. Sci.*, vol. 58, no. 10, pp. 1803–1809, 1995, doi: 10.1002/app.1995.070581019.

[98] M. A. Garrido and R. Font, “Pyrolysis and combustion study of flexible polyurethane foam,” *J. Anal. Appl. Pyrolysis*, vol. 113, pp. 202–215, 2015, doi: 10.1016/j.jaap.2014.12.017.

[99] D. Price, Y. Liu, G. J. Milnes, R. Hull, B. K. Kandola, and A. R. Horrocks, “An investigation into the mechanism of flame retardancy and smoke suppression by melamine in flexible polyurethane foam,” *Fire Mater.*, vol. 26, no. 4–5, pp. 201–206, 2002, doi: 10.1002/fam.810.

[100] M. Ravey and E. M. Pearce, “Flexible polyurethane foam. I. Thermal decomposition of a polyether-based, water-blown commercial type of flexible polyurethane foam,” *J. Appl. Polym. Sci.*, vol. 63, no. 1, pp. 47–74, 1997, doi: 10.1002/(sici)1097-4628(19970103)63:1<47::aid-app7>3.0.co;2-s.

[101] M. P. Luda, P. Nada, L. Costa, P. Bracco, and S. V. Levchik, “Relevant factors in scorch generation in fire retarded flexible polyurethane foams: I. Amino group reactivity,” *Polym. Degrad. Stab.*, vol. 86, no. 1, pp. 33–41, 2004, doi: 10.1016/j.polymdegradstab.2003.11.009.